

Ca²⁺-induced uncoupling of *Aplysia* bag cell neurons

Zahra Dargaei, Dominic Standage, Christopher J. Groten, Gunnar Blohm, and Neil S. Magoski

Department of Biomedical and Molecular Sciences, Physiology Graduate Program, Centre for Neuroscience Studies, Queen's University, Kingston, Ontario, Canada

Submitted 12 August 2014; accepted in final form 12 November 2014

Dargaei Z, Standage D, Groten CJ, Blohm G, Magoski NS. Ca²⁺-induced uncoupling of *Aplysia* bag cell neurons. *J Neurophysiol* 113: 808–821, 2015. First published November 19, 2014; doi:10.1152/jn.00603.2014.—Electrical transmission is a dynamically regulated form of communication and key to synchronizing neuronal activity. The bag cell neurons of *Aplysia* are a group of electrically coupled neuroendocrine cells that initiate ovulation by secreting egg-laying hormone during a prolonged period of synchronous firing called the afterdischarge. Accompanying the afterdischarge is an increase in intracellular Ca²⁺ and the activation of protein kinase C (PKC). We used whole cell recording from paired cultured bag cell neurons to demonstrate that electrical coupling is regulated by both Ca²⁺ and PKC. Elevating Ca²⁺ with a train of voltage steps, mimicking the onset of the afterdischarge, decreased junctional current for up to 30 min. Inhibition was most effective when Ca²⁺ entry occurred in both neurons. Depletion of Ca²⁺ from the mitochondria, but not the endoplasmic reticulum, also attenuated the electrical synapse. Buffering Ca²⁺ with high intracellular EGTA or inhibiting calmodulin kinase prevented uncoupling. Furthermore, activating PKC produced a small but clear decrease in junctional current, while triggering both Ca²⁺ influx and PKC inhibited the electrical synapse to a greater extent than Ca²⁺ alone. Finally, the amplitude and time course of the postsynaptic electrotonic response were attenuated after Ca²⁺ influx. A mathematical model of electrically connected neurons showed that excessive coupling reduced recruitment of the cells to fire, whereas less coupling led to spiking of essentially all neurons. Thus a decrease in electrical synapses could promote the afterdischarge by ensuring prompt recovery of electrotonic potentials or making the neurons more responsive to current spreading through the network.

electrical coupling; junctional current; calcium; protein kinase C; neuroendocrine cell

ELECTRICAL COUPLING via gap junctions is found in many cell types (Dermietzel and Spray 1993), including neurons, where it synchronizes activity (Bennett and Zukin 2004; Söhl et al. 2005; Spray and Bennett 1985). Like their chemical counterparts, electrical synapses are subjected to modulation by various second messengers and effectors (Lampe and Lau 2004; Neyton and Trautmann 1986; Peracchia 2004). One of the earliest described forms of regulation is the inhibition of gap junctions by increased intracellular Ca²⁺ (Spray and Bennett 1985), which was first reported by Loewenstein et al. (1967) in salivary glands of the midge *Chironomus*. Subsequently, this has been investigated in many nonneuronal and neuronal cells by intracellular injection of Ca²⁺ (De Mello 1975; Schirrmacher et al. 1996) or liberating Ca²⁺ with either pharmacological agents (Baux et al. 1978; Dahl and Isenberg 1980; Mus-

tonen et al. 2005) or cytoplasmic acidification (Spray et al. 1982; White et al. 1990).

Intracellular Ca²⁺ can modulate both vertebrate (Rao et al. 1987) and invertebrate (Baux et al. 1978; Pereda et al. 1998) neuronal coupling and likely acts through the activation of signal transduction pathways such as calmodulin (CaM) (Peracchia 2004) and CaM-kinases (Pereda et al. 1998). Gap junction proteins bind CaM directly, and some are phosphorylated by CaM-kinase II (Alev et al. 2008; Burr et al. 2005; Peracchia et al. 2000; Van Eldik et al. 1985). In the present study, we used the bag cell neurons of *Aplysia* to explore the Ca²⁺-dependent modulation of electrical synapses.

The bag cell neurons of the marine mollusk *Aplysia californica* are neuroendocrine cells located at the rostral end of the abdominal ganglion in two clusters of 200–400 neurons. They initiate reproduction through the secretion of egg-laying hormone during a lengthy and synchronous afterdischarge (Kaczmarek et al. 1978; Kupfermann and Kandel 1970; Pinsker and Dudek 1977; Rothman et al. 1983). This burst presents as a fast phase of firing (~5 Hz for ~1 min) followed by a slow phase of firing (~1 Hz for ~30 min). Synchrony is achieved through electrical coupling, both between neurons in a cluster as well as from one cluster to the other (Blankenship and Haskins 1979; Brown et al. 1989; Kaczmarek et al. 1979). The afterdischarge is accompanied by an increase in intracellular Ca²⁺ due to influx and release (Fisher et al. 1994; Michel and Wayne 2002). Furthermore, protein kinase C (PKC) is activated shortly after the onset of firing (Conn et al. 1989a; Wayne et al. 1999) and serves to potentiate Ca²⁺ channels (DeRiemer et al. 1985; Knox et al. 1992; Tam et al. 2009).

Here we performed whole cell recording on paired cultured bag cell neurons to show that Ca²⁺ influx through voltage-gated Ca²⁺ channels, or Ca²⁺ liberated from the mitochondria, attenuates electrical coupling in a CaM-kinase-dependent fashion. Triggering PKC coincident with Ca²⁺ entry inhibits electrical synapses to an even greater extent, although never to the point of decoupling. In the intact cluster, this may bolster excitability by decreasing the net leakiness of a given neuron. Ca²⁺ influx also decreases the amplitude and duration of electrotonic transmission, which may improve synchrony by preventing lengthy responses and out-of-phase postsynaptic action potentials. Hence modulation of electrical coupling may help maintain and augment the release of reproductive hormone.

MATERIALS AND METHODS

Animals and cell culture. Adult *A. californica* (a hermaphrodite) weighing 150–500 g were obtained from Marinus (Long Beach, CA), housed in an ~300-liter aquarium containing continuously circulating, aerated artificial seawater (ASW) (Instant Ocean; Aquarium Systems, Mentor, OH) at 14–16°C on a 12:12-h light-dark cycle, and

Address for reprint requests and other correspondence: N. S. Magoski, Dept. of Biomedical and Molecular Sciences, Queen's Univ., 4th Floor, Botterell Hall, 18 Stuart St., Kingston, ON, K7L 3N6, Canada (e-mail: magoski@queensu.ca).

fed romaine lettuce five times per week. Experiments were approved by the Queen's University Animal Care Committee (protocols Magoski-100323 and Magoski-100845).

For primary culture of isolated bag cell neurons, animals were anesthetized by an injection of isotonic MgCl₂ (50% of body wt) and the abdominal ganglion was removed and treated with dispase II (13.3 mg/ml; 165859; Roche Diagnostics, Indianapolis, IN) dissolved in tissue culture (tc)ASW (composition in mM: 460 NaCl, 10.4 KCl, 11 CaCl₂, 55 MgCl₂, and 15 HEPES, with 1 mg/ml glucose, 100 U/ml penicillin, and 0.1 mg/ml streptomycin, pH 7.8 with NaOH) for 18 h at 22°C. The ganglion was then rinsed in tcASW for 1 h, and the bag cell neuron clusters were dissected from their surrounding connective tissue. With a fire-polished glass Pasteur pipette, neurons were dissociated by gentle trituration and dispersed in tcASW onto 35 × 10-mm polystyrene tissue culture dishes (353001; Falcon Becton-Dickinson, Franklin Lakes, NJ). Neurons were paired by moving tcASW in or out of the pipette to push or pull a free neuron into contact with a neuron already adhered to the dish. Neurons were plated with either their somata (soma-soma) or primary neurites (neurite-neurite) in contact. For Ca²⁺ imaging (see below), single neurons were plated. Cultures were maintained in a 14°C incubator in tcASW and used for experimentation within 2–4 days. Salts were obtained from Fisher (Ottawa, ON, Canada), ICN (Aurora, OH), or Sigma-Aldrich (Oakville, ON, Canada).

Whole cell voltage- and current-clamp recording. Recordings of membrane potential or current were made from cultured bag cell neurons with two EPC-8 amplifiers (HEKA Electronics, Mahone Bay, NS, Canada) and the tight-seal whole cell method. Microelectrodes were pulled from 1.5-mm-external diameter/1.12-mm-internal diameter borosilicate glass capillaries (TW150F-4; World Precision Instruments, Sarasota, FL) and had a resistance of 1–2 MΩ when filled with our standard intracellular saline [composition in mM: 500 K⁺-aspartate, 70 KCl, 1.25 MgCl₂, 10 HEPES, 11 glucose, 10 glutathione, 5 EGTA, 5 ATP (grade 2, disodium salt; A-3377, Sigma-Aldrich), and 0.1 GTP (type 3, disodium salt; G-8877, Sigma-Aldrich); pH 7.3 with KOH]. The free Ca²⁺ concentration was set at 300 nM by adding 3.75 mM CaCl₂, as calculated by WebMaxC (<http://web.stanford.edu/~cpatton/webmaxcs.htm>). In two separate sets of experiments, an intracellular saline with either 0 mM EGTA and no added Ca²⁺ or 20 mM EGTA and 35 nM free Ca²⁺ (4.14 mM added CaCl₂) as well as 40 mM EGTA and 15 nM free Ca²⁺ (4.14 mM added CaCl₂) was used. Neuronal pairs were usually dialyzed for 30 min under voltage clamp at –60 mV before experimentation. Our lab has found that this length of time is necessary to ensure that, as much as possible, the intracellular ions are exchanged with those of the pipette (White and Magoski 2012). In turn, this avoided any potential run-up or rundown of junctional current that could arise from differences or ongoing changes in intracellular ion concentration.

Recordings were performed in normal (n)ASW (composition as per tcASW, but with glucose and antibiotics omitted). The standard intracellular saline had a calculated liquid junction potential of 15 mV vs. ASW, which was corrected by off-line subtraction. For a subset of experiments, some pairs were bathed in Ca²⁺-free ASW (composition as per nASW but with no added Ca²⁺, 66 mM Mg²⁺, and 0.5 mM EGTA). Pipette junction potentials were nulled immediately before seal formation. After membrane rupture, pipette and neuronal capacitive currents were canceled and the series resistance (3–5 MΩ) was compensated to 70–80% and monitored throughout the experiment. Input signals were filtered at 1 kHz (for current) and 3 kHz (for voltage) by the EPC-8 Bessel filter and sampled at 2 kHz with an IBM-compatible personal computer, a Digidata 1322A analog-to-digital converter (Molecular Devices; Sunnyvale, CA), and the Clampex acquisition program of pCLAMP 8.1 (Molecular Devices). Clampex was used to control the membrane potential under voltage clamp and to inject current steps under current clamp; in addition, neurons were manually current-clamped to set membrane potentials by delivering constant bias current with the EPC-8 V-hold. Most data pre-

sented here are for junctional current, which is the current provided by the amplifier to maintain the voltage clamp of the postsynaptic neuron at –60 mV, after creation of a voltage difference across the gap junction by a voltage step (to –90 mV) to the presynaptic neuron.

Ca²⁺ imaging. For Ca²⁺ imaging, single neurons were dialyzed with standard intracellular saline supplemented with 1 mM fura-PE3 (K⁺ salt; 0110, Teflabs, Austin, TX) (Vorndran et al. 1995). Imaging was performed with a TS100-F inverted microscope (Nikon) equipped with a Nikon Plan Fluor ×20 (numerical aperture = 0.5) objective. The light source was a 75-W Xe arc lamp and a multiwavelength DeltaRAM V monochromatic illuminator (Photon Technology International, London, ON, Canada) coupled to the microscope with a UV-grade liquid-light guide. Excitation wavelengths were 340 and 380 nm and delivered through a computer-controlled shutter with a Photon Technology International computer interface and EasyRatio Pro software 1.10 (Photon Technology International). During acquisition, the shutter remained open and emitted light passed through a 400-nm long-pass dichroic mirror and a 510/40-nm emission barrier filter before being detected by a Cool SNAP HQ2 charge-coupled device camera (Photometrics, Tucson, AZ). The camera gain was maximized and the exposure time set at 1 s for both 340- and 380-nm excitation wavelengths. Fluorescence intensities were sampled at 0.5 Hz using regions of interest measured over the somata at approximately the midpoint of the vertical focal plane and one-half to three-quarters of the cell diameter, then averaged eight frames per acquisition. The ratio of the emission after 340- and 380-nm excitation (340/380) was taken to reflect free intracellular Ca²⁺ (Grynkiewicz et al. 1985) and saved for subsequent analysis. Image acquisition, emitted light sampling, and ratio calculations were performed with EasyRatio Pro.

Reagents and drug application. Solution changes were accomplished by using a calibrated transfer pipette to exchange the bath (tissue culture dish) solution. Drugs were introduced by initially removing a small volume (~75 μl) of saline from the bath, combining that with an even smaller volume (<10 μl) of drug stock solution, and then reintroducing that mixture back into the bath. Care was taken to pipette near the side of the dish and as far away as possible from the neurons. Phorbol 12-myristate 13-acetate (PMA; P-8139, Sigma-Aldrich), cyclopiazonic acid (CPA; C-1530, Sigma-Aldrich), carbonyl cyanide *p*-trifluoromethoxyphenylhydrazone (FCCP; 21857, Sigma-Aldrich), KN-62 (I-2142, Sigma-Aldrich), KN-92 (422709, Calbiochem/EMD Millipore, Billerica, MA), KN-93 (422708, Calbiochem), and ryanodine (559276, Calbiochem) were dissolved as stocks in dimethyl sulfoxide (DMSO; BP231-1, Fisher). The maximal final concentration of DMSO ranged from 0.05% to 0.5% (vol/vol), which in control experiments both here and in prior work from our laboratory had no effect on holding current, membrane conductance, or junctional current (Dargaei et al. 2014; Hickey et al. 2010, 2013; Kachoei et al. 2006; Tam et al. 2011).

Data analysis. Most analysis involved cell pairs designated as *neuron 1* and *neuron 2*, based on being recorded with the left and right amplifier, with membrane potentials and membrane currents specified as V1, V2, I1, and I2, respectively. The Clampfit (8.1 or 10.2) analysis program of pCLAMP was used to determine the amplitude and time course of membrane current or voltage. For current, vertical cursors were placed along the baseline, both prior to any voltage step and when the junctional current had reached steady-state at 20–30 ms before the end of the step to –90 mV. Some measurements were made by using the horizontal cursor as a guide to effectively adjacently average the two regions and find average current levels; the difference between the two was then taken as the current change. Measurements were also made by using two vertical cursors placed to span the 10 ms immediately prior to the current change evoked by the step, while an additional two cursors were positioned 20–30 ms before the end of the junctional current and just before the end of the junctional current, respectively. Clampfit then calculated the average current between each pair of cursors, and the difference between the averages was taken as the current change. The percent

change in junctional current following Ca²⁺ influx due to stimulation or the addition of a drug was calculated by comparing the subsequent current to control. The area of the electrotonic potential (ETP) was measured by placing cursors at the onset of the ETP and at the steady-state voltage after the ETP, i.e., when the postsynaptic membrane potential had fully returned to the pre-ETP baseline. The difference between the two cursors was taken as the region of the ETP, under which the ETP area was calculated. The time to recovery of the ETP was determined by placing cursors at peak of the ETP and steady-state voltage after ETP recovery and then taking the difference. For intracellular Ca²⁺, analysis compared the absolute change in the steady-state value of the baseline 340/380 from regions that had reached a peak or new steady-state during long (5 Hz for 1 min) and short (1 Hz for 5 min) train-stimuli. Averages of the baseline and peak regions were determined by eye or adjacent averaging.

Statistics were performed with Prism 6.01 (GraphPad Software, La Jolla, CA) or InStat 3.1 (GraphPad). Summary data were compiled as bar graphs with Prism and are presented as means \pm SE. The Kolmogorov-Smirnov method was used to test data sets for normality. Student's unpaired *t*-test was used to test for differences between two means from normally distributed data, while the Wilcoxon matched-pairs signed-ranks test was used for two means from not normally distributed data. To test for differences between multiple means, a standard one-way analysis of variance (ANOVA) was used, followed by the Dunnett multiple-comparisons test for examining differences between control and remaining groups or the Tukey-Kramer multiple-comparisons test for examining differences between all groups. Data were considered statistically significant if the two-tailed *P* value was <0.05 .

Model development. A model network of gap junction-connected neurons was constructed with equations solved with Euler's method written in MATLAB (7.6; MathWorks, Natick, MA). The network was comprised of 100 Hodgkin-Huxley-type neurons (Hodgkin and Huxley 1952; Izhikevich 2007), each described by

$$\begin{aligned} C dV/dt &= -g_L(V - E_L) - g_K n^4(V - E_K) - g_{Na} m^3 h(V - E_{Na}) \\ &\quad - I_{Ca} - I_{syn}(I) \\ dn/dt &= [n_\infty(V) - n]/\tau_n(V) \\ dm/dt &= [m_\infty(V) - m]/\tau_m(V) \\ dh/dt &= [h_\infty(V) - h]/\tau_h(V) \end{aligned}$$

where $C = 1 \mu\text{F}/\text{cm}^2$ is the membrane capacitance of the neuron; V is the membrane potential; $g_L = 0.3 \text{ mS}/\text{cm}^2$, $g_K = 36 \text{ mS}/\text{cm}^2$, and $g_{Na} = 110 \text{ mS}/\text{cm}^2$ are the conductances for leakage, K⁺, and Na⁺ currents, respectively; $E_L = -54.4 \text{ mV}$, $E_K = -77 \text{ mV}$, and $E_{Na} = 50 \text{ mV}$ are their respective reversal potentials; n and m are gating variables for activation of the K⁺ and Na⁺ currents, respectively; h is a gating variable for inactivation of the Na⁺ current; I_{Ca} is a persistent calcium current; and I_{syn} is synaptic current mediated by extrinsic chemical synapses and intrinsic electrical synapses. For the gating variables $x \in \{n, m, h\}$,

$$x_\infty(V) = \alpha_x / (\alpha_x + \beta_x); \tau_x(V) = 1 / (\alpha_x + \beta_x) \quad (2)$$

where $x_\infty(V)$ is the steady-state activation (n and m) or deactivation (h) function and $\tau_x(V)$ is its time constant. For each activation or deactivation variable, the functions α and β describe the transition rates between open and closed states, given by

$$\begin{aligned} \alpha_n(V) &= 0.01(V + 55) / \{1 - \exp[-(V + 55)/10]\}, \\ \beta_n(V) &= 0.125 \cdot \exp[-(V + 65)/80] \\ \alpha_m(V) &= 0.1(V + 40) / \{1 - \exp[-(V + 40)/10]\}, \\ \beta_m(V) &= 4 \cdot \exp[-(V + 65)/18] \\ \alpha_h(V) &= 0.07 \cdot \exp[-(V + 65)/20], \\ \beta_h(V) &= 1 / \{1 + \exp[-(V + 35)/10]\} \end{aligned} \quad (3)$$

The persistent calcium current I_{Ca} is a high-voltage-activated (L-like) current, described by

$$\begin{aligned} I_{Ca} &= G_{Ca} y(V - E_{Ca}) \\ dy/dt &= [y_\infty(V) - y]/\tau_y \\ y_\infty &= 1 / [1 + \exp(V - \theta_y)/z] \end{aligned} \quad (4)$$

where $g_{Ca} = 4 \text{ ms}/\text{cm}^2$ is its conductance strength, $E_{Ca} = 60 \text{ mV}$ is its reversal potential, and y gates its activation. The steady-state value of y is given by y_∞ , where $\theta_y = -10 \text{ mV}$ is the voltage at half-activation and $z = -6 \text{ mV}$ determines the slope of the function (Carlin et al. 2000).

Synaptic current I_{syn} is comprised of acetylcholine receptor-mediated current I_{ACh} and gap junction-mediated current I_{gap} . The former is given by $I_{ACh} = g_{ACh} x_{ACh}(V - E_{ACh})$, where $g_{ACh} = 0.05 \text{ ms}/\text{cm}^2$ is its conductance strength, $E_{ACh} = 0 \text{ mV}$ is its reversal potential, and receptor activation is described by

$$dx_{ACh}/dt = -x_{ACh}/\tau_{ACh} + \delta(t - t_f) \quad (5)$$

where $\tau_{ACh} = 25 \text{ ms}$ is the time constant of decay, δ is the Dirac delta function, and t_f is the time of firing of a presynaptic neuron. For the gap junction-mediated current I_{gap} , the coupling between neurons followed a "nearest neighbor" approach:

$$I_{gap}^j = g_{gap}(V^{j+1} - 2V^j + V^{j-1}) \quad (6)$$

where $j = 2 : 99$ is the index of an individual neuron and g_{gap} is its conductance strength (Ermentrout et al. 2004). For the special cases of $j = 1$ and $j = 100$, the neurons were only coupled to one other cell. Presynaptic spikes were simulated by periodic spike trains at 20 Hz, provided to *neurons 35–64*.

RESULTS

Cultured pairs of bag cell neurons show electrical coupling. Previous morphological and electrophysiological studies of bag cell neurons in the intact cluster showed that the bag cell neurons are electrically coupled (Blankenship and Haskins 1979; Brown et al. 1989; Kaczmarek et al. 1979). To study these synapses under more controlled conditions, we disassociated bag cell neurons and brought them into contact at either the somata (Fig. 1A) or the neurites (Fig. 1B). After 2–4 days in culture, ~80% of pairs usually exhibited electrical coupling. Whole cell recording, in either voltage or current clamp, was used in all cases. Unless stated otherwise, recordings were made in nASW as the extracellular solution and a K⁺-Asp-based intracellular saline in the pipette (see MATERIALS AND METHODS for details). Cells were designated as *neuron 1* and *neuron 2*, with *neuron 1* always as the presynaptic cell and *neuron 2* the postsynaptic cell, the rationale being that electrical coupling between cultured bag cell neurons is non-rectifying and has the same magnitude when either *neuron 1* or *neuron 2* serves in a presynaptic role (Dargaei et al. 2014).

To confirm the existence of electrical synapses between cultured bag cell neurons, a 1-nA, 5-s depolarizing current was injected into one neuron under current clamp, which usually elicited a train of nonaccommodating action potentials over the duration of the stimulus ($n = 25$) (Fig. 1C). Both the steady-state depolarization and action potentials in the stimulated neuron generated depolarization and ETPs in the second neuron. In some cases, electrotonic transmission was able to recruit the coupled cell and provoke postsynaptic action potentials ($n = 9$ of 25).

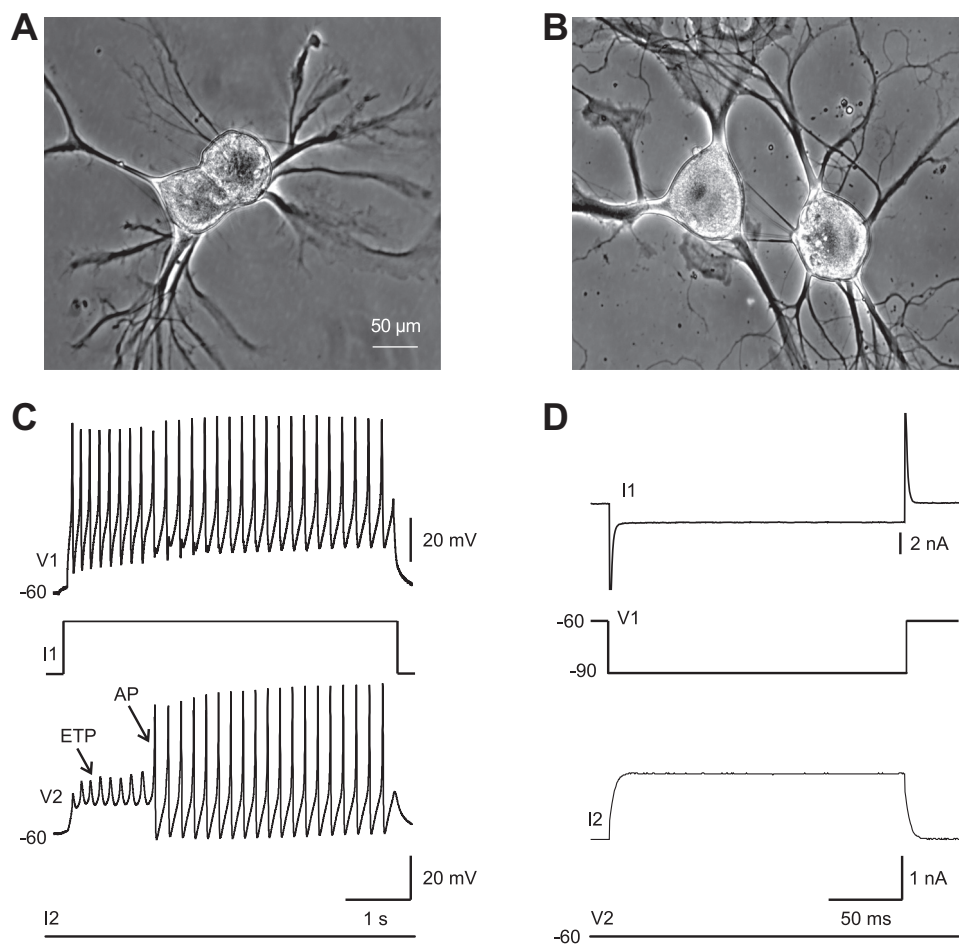


Fig. 1. Cultured pairs of bag cell neurons are electrically coupled. *A* and *B*: phase-contrast photomicrographs of paired bag cell neurons. The soma-soma configuration (*A*) is between cells cultured for 2 days, while the neurons making neurite-to-neurite contact (*B*) are in vitro for 3 days. Scale bar applies to both pictures. *C*: whole cell current-clamp recording from a pair of coupled bag cell neurons. A 1-nA, 5-s depolarizing current injection into *neuron 1* (I1) evokes action potentials in *neuron 1* (V1), resulting in steady-state depolarization and electrotonic potentials (ETPs) in *neuron 2* (V2) that reach threshold to generate action potentials (APs). Time base applies to all traces. *D*: under whole cell voltage clamp, a pair of coupled bag cell neurons is held at -60 mV. Changing the voltage of 1 cell to -90 mV (V1) for 200 ms elicits both inward membrane current in *neuron 1* (I1) and junctional current in *neuron 2* (I2). The outward current of I2 is the current required to keep the second cell voltage clamped at -60 mV (V2) in the face of a potential difference across the gap junction and thus represents the junctional current. Time base applies to all traces.

For the majority of the experiments described in RESULTS, we measured junctional current under voltage clamp by applying a potential difference to *neuron 1* and measuring the corresponding current in *neuron 2*. From a holding potential of -60 mV for both cells, a 200-ms voltage step to -90 mV in *neuron 1*, while continuing to hold *neuron 2* at -60 mV, induced current in both neurons. Figure 1*D* provides an example of how this hyperpolarizing pulse caused an inward current in the stimulated neuron and, when cells were electrically coupled, evoked an outward current in the unstimulated neuron. Because the second neuron was maintained at -60 mV, the outward current corresponds to current flowing across the electrical synapse.

Increased intracellular Ca²⁺ inhibits the electrical synapse. Prior work indicated that the afterdischarge resulted in an increase in intracellular Ca²⁺ due to both voltage-gated influx and release from intracellular stores (Fisher et al. 1994; Michel and Wayne 2002). Ca²⁺ has been shown to inhibit gap junctions in both nonneuronal (Loewenstein et al. 1967; Spray et al. 1982) and neuronal (Baux et al. 1978; Rao et al. 1987) cells; however, it is relatively rare to find cases of Ca²⁺ channels being the source of the rise in Ca²⁺. Thus we examined whether Ca²⁺ influx, produced by a train-stimulus of 75-ms pulses from -60 to 0 mV at 5 Hz for 1 min and then 1 Hz for 5 min, which mimics the fast and early slow phases of the afterdischarge, respectively, suppresses junctional current.

Electrically coupled cultured bag cell neurons were voltage-clamped, and the junctional current was measured in the postsynaptic neuron (Fig. 2*A*, inset) after a 30-min period to

allow for full dialysis. When neurons were not stimulated ($n = 6$), junctional current showed little change over time (Fig. 2*A*). However, delivering the combined train-stimulus to both neurons after 30 min of dialysis caused an $\sim 30\%$ decrease in junctional current (Fig. 2*B*) ($n = 7$). To confirm that Ca²⁺ was inhibiting electrical communication, extracellular Ca²⁺ was removed by substituting with Mg²⁺. With no Ca²⁺ in the bath ($n = 7$), the train-stimulus failed to alter the junctional current (Fig. 2*C*). The difference in the percent change in junctional current for control vs. Ca²⁺-free conditions was not significant; however, the change seen after Ca²⁺ influx was significantly different from both control and Ca²⁺-free conditions (Fig. 2*D*).

We also examined the time course of the change to intracellular Ca²⁺ in response to the 5-Hz, 1-min then 1-Hz, 5-min stimulus in fura-PE3-loaded cultured bag cell neurons from a holding potential of -60 mV under voltage clamp. There was an immediate and robust Ca²⁺ elevation with delivery of the 5-Hz train, followed by a less substantial plateau during the 1-min train (Fig. 2, *E* and *F*). Based on a comparison with prior Ca²⁺ measurements made by Fisher et al. (1994) in bag cell neurons with Ca²⁺-sensitive electrodes, we estimated that the ~ 0.4 -unit (340/380) change during the 5-Hz stimulus and the 0.175 unit change during 1-Hz stimulus translated roughly to deltas of 400 nM and 200 nM Ca²⁺, respectively, rendering a shift in Ca²⁺ from a baseline of ~ 200 – 300 nM to a peak of ~ 600 – 700 nM and a plateau of ~ 400 – 500 nM.

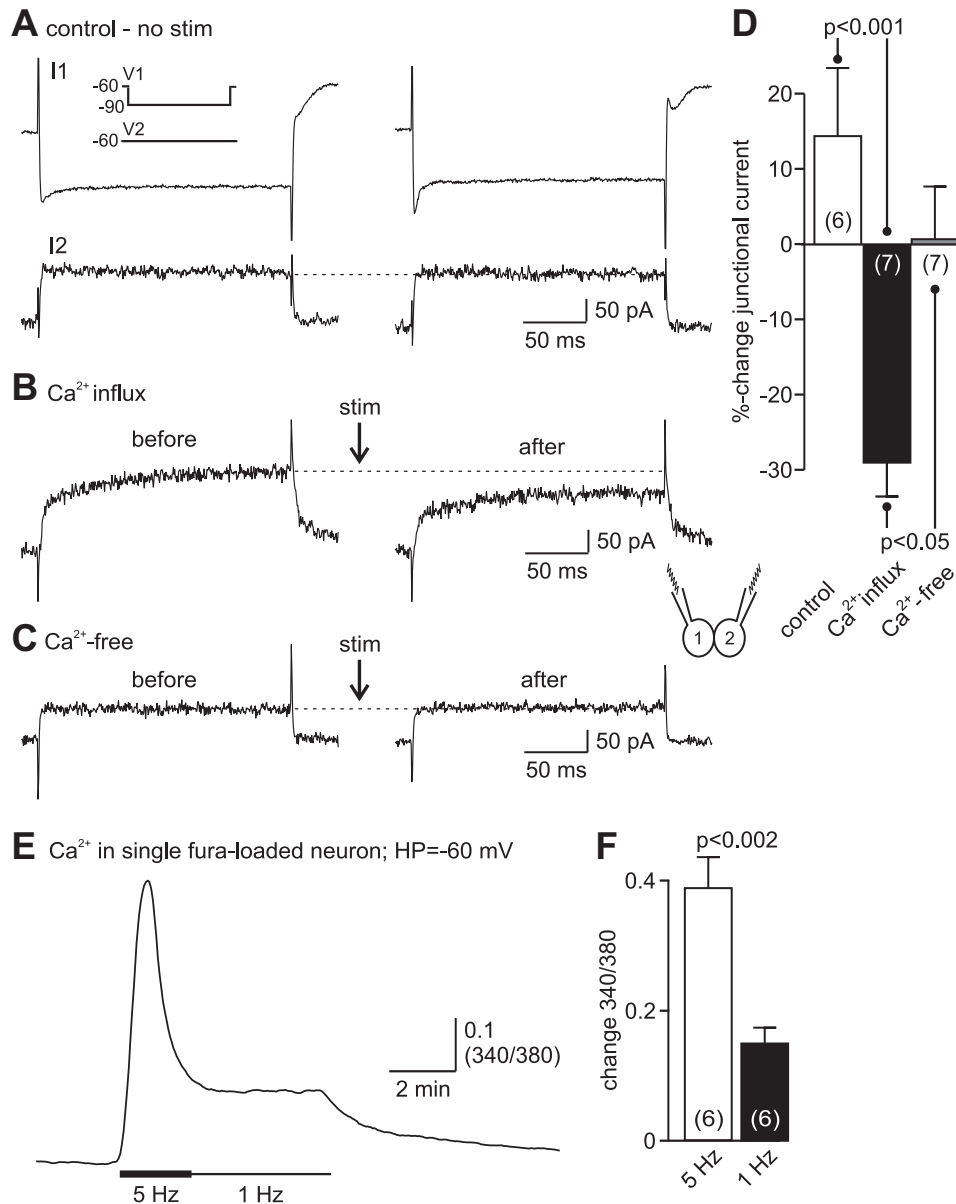


Fig. 2. Elevation of intracellular Ca²⁺ decreases junctional current. **A**: neurons are whole cell voltage-clamped at -60 mV in normal artificial seawater (nASW) with standard K⁺-Asp-based intracellular saline for 30 min to ensure complete dialysis. The voltage change in *neuron 1* produces membrane current in *neuron 1* (I1) and junctional current in *neuron 2* (I2). *Inset* shows the step voltage to assay junctional current. Scale bars apply to both traces. A dashed line extending from the end of the initial junctional current (I2, *left*) is placed at the estimated steady-state level to aid in comparison with the subsequent trace (*right*). **B**: Ca²⁺ influx, produced by simultaneously delivering to both cells (stim) a train of 75-ms pulses from -60 to 0 mV at 5 Hz for 1 min followed by 1 Hz for 5 min decreases the junctional current (after) compared with the initial response (before). The altered junctional current is recorded immediately after stimulation. For **B** and **C** only the junctional current (I2) is presented. *Inset* shows a pair of neurons with stimulation to both pipettes. Scale bars apply to both traces. **C**: in a Ca²⁺-free extracellular saline, where Mg²⁺ is substituted for Ca²⁺, the train-stimulus does not change the junctional current. Scale bars apply to both traces. **D**: summary graph showing that the % change in junctional current significantly decreases after stimulation in the presence of extracellular Ca²⁺ vs. both the unstimulated control and neurons stimulated in Ca²⁺-free solution ($F_{2,17} = 11.83$, $P < 0.05$, ANOVA; Tukey-Kramer multiple-comparisons test). For this and subsequent bar graphs, the n value (typically no. of pairs of cultured bag cell neurons) is shown in parentheses within or just above or below individual bars. **E**: measurement of intracellular Ca²⁺ in a single cultured bag cell neuron filled with fura-PE3. The neuron is voltage-clamped at a holding potential (HP) of -60 mV and, after 15 min of dialysis to dye-load, the stimulation train is delivered (as per **B** and **C**). The change in the ratio of the emission following 340 and 380 nm excitation (340/380) reflects elevated free intracellular Ca²⁺. During the 5-Hz, 1-min stimulus, the Ca²⁺ presents a large-amplitude component that declines to a stable elevation over the course of the 1-Hz, 5-min stimulus. **F**: group data comparing the change in 340/380, taken from prestimulus baseline to the peak of the response at 5 Hz and the plateau at 1 Hz, show a significant difference between the 2 frequencies (unpaired Student's t -test).

Synchronous stimulation is most effective at inhibiting electrical coupling. Closure of gap junctions has been reported to require the increase of cytosolic Ca²⁺ to a specific threshold (Rose and Loewenstein 1976). Therefore we examined whether a Ca²⁺ rise in only one cell from a pair of cultured bag

cell neurons was sufficient to inhibit the electrical synapse. Subsequent to a 30-min dialysis under voltage clamp, junctional current was induced (Fig. 3A, *inset*). As a control, the train-stimulus was simultaneously delivered to both neurons ($n = 5$), which resulted in an ~25% decrease in coupling that

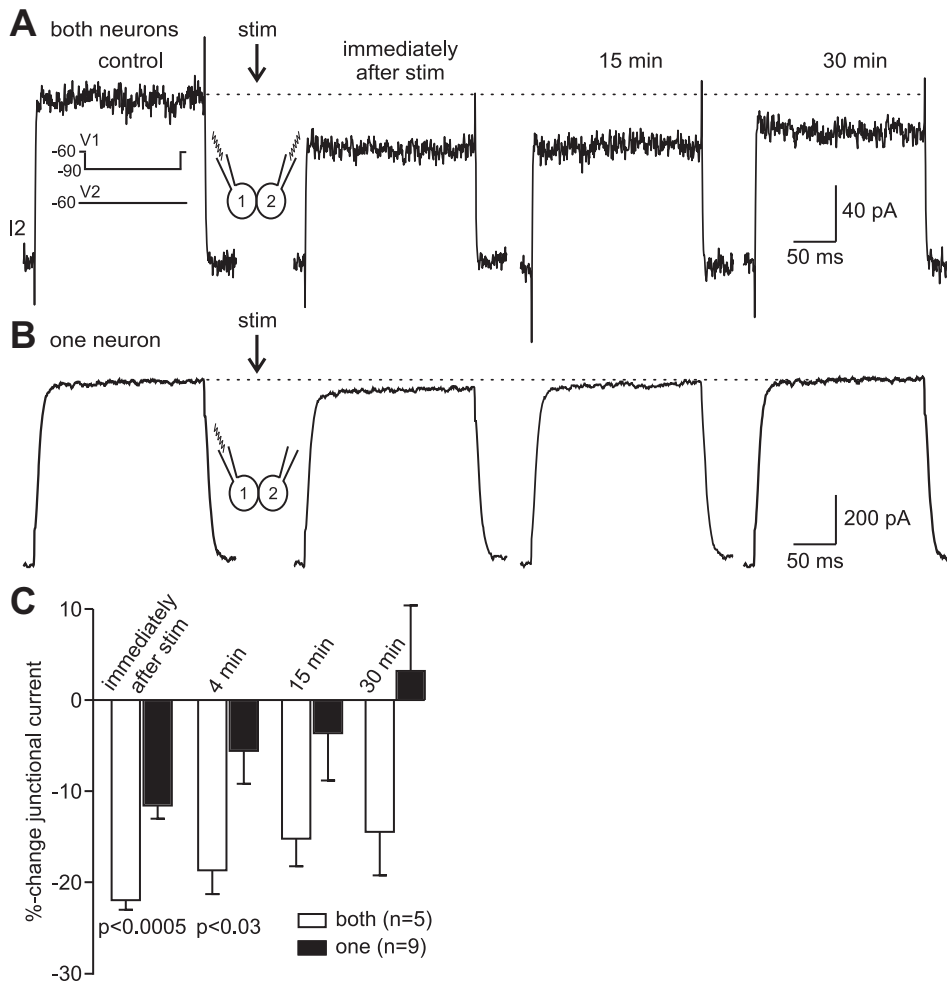


Fig. 3. Inhibition of junctional current is most effective when Ca²⁺ entry occurs in both neurons. *A*: intracellular Ca²⁺ elevation following delivery to both neurons (stim, inset) of the train-stimulus decreases junctional current (I₂) for up to 30 min. Only the junctional current is shown. Inset shows the voltage protocol to elicit junctional current. Scale bars apply to all time points. *B*: when the train-stimulus is delivered to just 1 neuron in the pair (inset), lowering of the junctional current is seen only immediately after stimulation. The gap junctions do not stay closed over time, and the junctional current recovers by 30 min. Scale bars apply to all time points. *C*: summary graph comparing % change in junctional current. A Ca²⁺ rise in both neurons reduces the junctional current, but elevating Ca²⁺ in only 1 cell results in a smaller effect that returns to baseline by 15 min. The difference between the stimulation conditions is significant immediately and 4 min after the train (unpaired Student's *t*-test at each time point).

lasted for up to 30 min (Fig. 3*A*). However, giving the same train-stimulus only to neuron 1, while keeping neuron 2 at -60 mV throughout ($n = 9$), caused a smaller inhibition of $\sim 10\%$ that decayed to no change by 30 min (Fig. 3*B*). When the change in junctional current following stimulation of both neurons was compared to that produced by stimulating just one neuron, the level of uncoupling was found to be significantly greater immediately after Ca²⁺ influx and 4 min later (Fig. 3*C*).

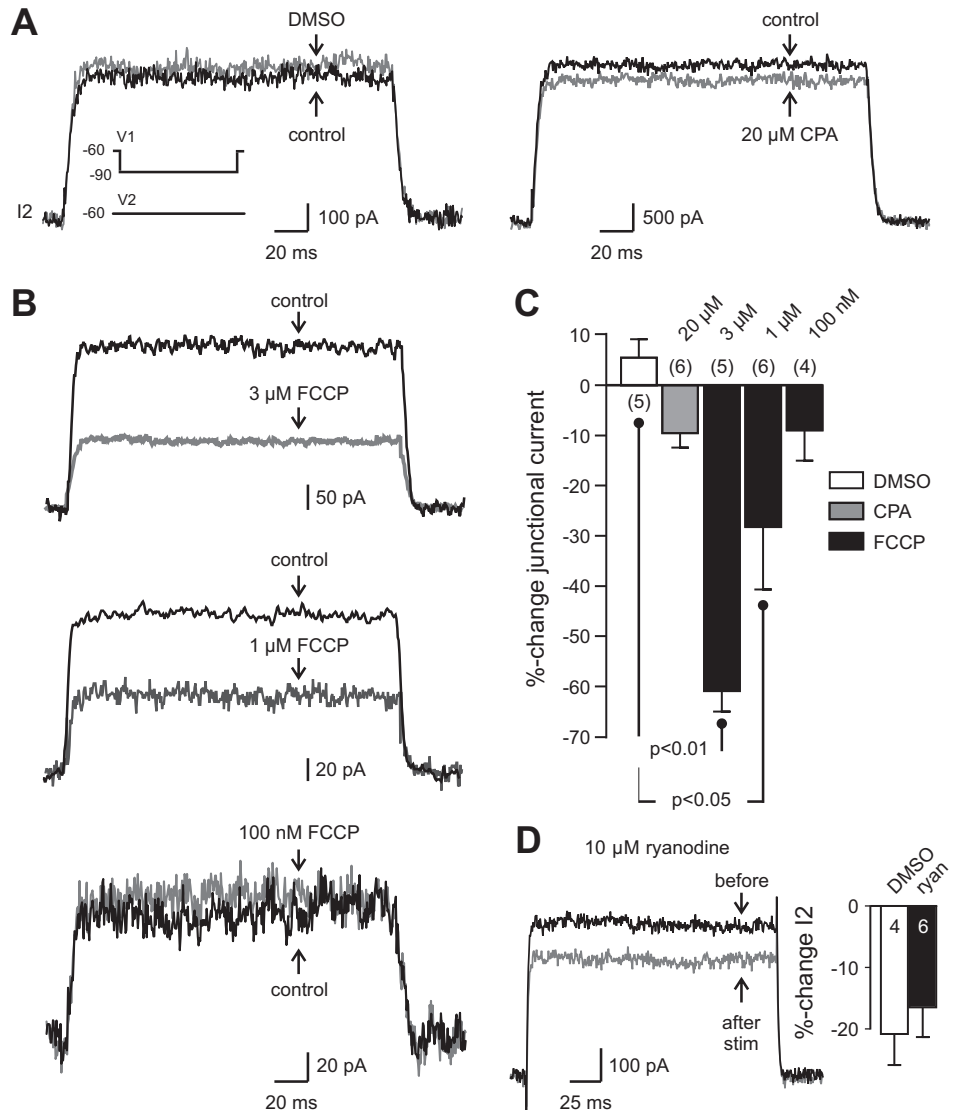
Depletion of mitochondrial Ca²⁺ attenuates junctional current. Fisher et al. (1994) demonstrated that Ca²⁺-induced Ca²⁺ release occurred from intracellular stores during the slow phase of the afterdischarge, and this required an interaction between mitochondria and endoplasmic reticulum (Geiger and Magoski 2008; Groten et al. 2013). As such, EGTA and Ca²⁺ were removed from the pipette solution (to avoid influencing store-derived Ca²⁺) and the impact of Ca²⁺ liberation from either the endoplasmic reticulum or mitochondria on electrical coupling was examined. After a 30-min dialysis, junctional current was measured from pairs of cultured bag cell neurons (Fig. 4*A*, inset) before and after the addition of DMSO (the vehicle) or Ca²⁺-liberating drugs. Introduction of either DMSO ($n = 5$) or 20 μ M CPA ($n = 6$), an agent that depletes endoplasmic reticulum Ca²⁺ by inhibiting the Ca²⁺-ATPase (Seidler et al. 1989), produced no substantial change in junctional current compared with control (Fig. 4*A*, left and right). However, FCCP, a protonophore that collapses the mitochon-

drial membrane potential and causes Ca²⁺ to exit (Heytler and Prichard 1962), inhibited junctional current in a concentration-dependent fashion (Fig. 4*B*) when applied at 100 nM ($n = 4$), 1 μ M ($n = 6$), or 3 μ M ($n = 5$). The reduction was significantly greater when the two higher concentrations were compared to DMSO (Fig. 4*C*). Our prior work showed that the Ca²⁺ liberated by FCCP activated a cation current, which required ~ 5 min to recover (Hickey et al. 2010); hence we measured junctional current 10 min after FCCP.

To more rigorously test the role of endoplasmic reticulum Ca²⁺, coupled pairs were subjected to the train-stimulus after a 20- to 30-min treatment with 10 μ M ryanodine or DMSO. Micromolar levels of ryanodine, an antagonist of the endoplasmic reticulum Ca²⁺-activated Ca²⁺ channel (Meissner 1985), have been shown by our laboratory to prevent Ca²⁺-induced Ca²⁺ release from cultured bag cell neurons (Geiger and Magoski 2008). Nevertheless, blocking any potential Ca²⁺ release during stimulation did not impact the ability of Ca²⁺ influx to inhibit junctional current, with DMSO and ryanodine presenting no significant difference in the level of uncoupling brought about by stimulation (Fig. 4*D*).

Sustained inhibition of electrical synapses depends on intracellular Ca²⁺. To confirm whether the prolonged decrease in coupling after the train-stimulus was due to changes in intracellular Ca²⁺, the Ca²⁺ buffering capacity of the pipette solution was enhanced by replacing the

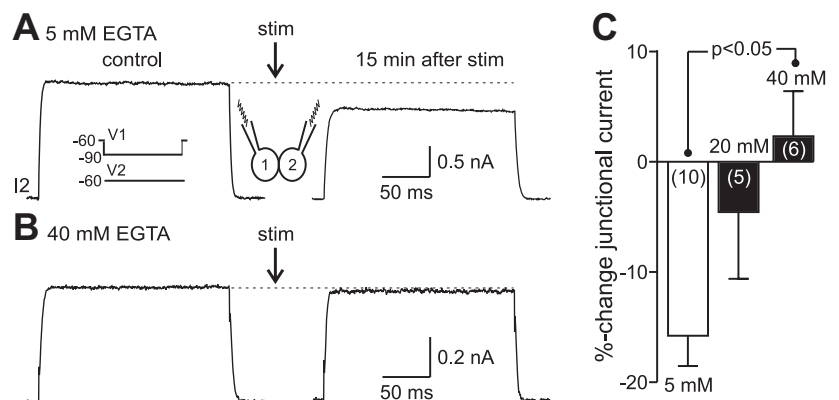
Fig. 4. Depletion of mitochondria Ca²⁺, but not endoplasmic reticulum Ca²⁺, inhibits junctional communication. **A:** neurons are voltage-clamped at -60 mV and dialyzed for 30 min with 0 mM EGTA and no added Ca²⁺ in the intracellular saline. *Left:* introducing dimethyl sulfoxide (DMSO, vehicle) produces little change in junctional current. *Inset* depicts the command voltage to evoke junctional current in neuron 2 (I2). *Right:* similarly, liberating endoplasmic reticulum Ca²⁺ with 20 μ M cyclopiazonic acid (CPA), an inhibitor of the endoplasmic reticulum Ca²⁺-ATPase, does not appreciably alter the junctional current (gray trace) compared with control taken prior to CPA (black trace). **B:** addition of 3 μ M carbonyl cyanide *p*-trifluoromethoxyphenylhydrazone (FCCP) to the bath collapses the mitochondrial membrane potential and results in a Ca²⁺ leak into the cytosol from this organelle. This inhibits junctional current 10 min after FCCP is applied. The FCCP-induced inhibition is concentration dependent, as 1 μ M and 100 nM have a progressively weaker effect on the electrical synapse. Time base applies to all 3 sets of traces. **C:** summary data of the mean change from control in junctional current after DMSO (vehicle), CPA, or FCCP. The junctional current is significantly reduced by higher concentrations of FCCP, but not CPA, vs. DMSO ($F_{2,21} = 11.59$, $P < 0.001$, ANOVA; Dunnett multiple-comparisons test). **D:** a neuronal pair incubated for 20 min in 10 μ M ryanodine, a blocker of the endoplasmic reticulum Ca²⁺ channel, still displays a Ca²⁺ influx-dependent drop in junctional current (I2) after the train-stimulus (gray trace) compared with just before (black trace). *Inset:* summary data of DMSO (vehicle) vs. ryanodine shows no significant difference between the 2 conditions (unpaired Student's *t*-test).



standard intracellular saline containing 5 mM EGTA to one using either 20 mM or 40 mM EGTA (Naraghi 1997) (see MATERIALS AND METHODS for details). Neurons were dialyzed at -60 mV for 30 min, and the junctional current was studied before and after Ca²⁺ influx (Fig. 5A, *inset*). In control, where standard intracellular saline was in the pipettes ($n = 10$), the train-stimulus caused an $\sim 15\%$ decrease

in junctional current that lasted for at least 15 min (Fig. 5A). Subsequent to dialysis with 40 mM EGTA intracellular saline, the same stimulus failed to reduce junctional current and yielded an $\sim 5\%$ increase after 15 min (Fig. 5B) ($n = 6$); the difference between 5 mM and 40 mM EGTA was significant (Fig. 5C). Using 20 mM EGTA-containing intracellular saline ($n = 5$) resulted in an $\sim 5\%$ reduction in

Fig. 5. Buffering Ca²⁺ with high intracellular EGTA prevents uncoupling. **A:** recording of junctional current between a pair of electrically coupled bag cell neurons dialyzed for 30 min with intracellular saline containing 5 mM EGTA. The junctional current (I2) shows a decrease after Ca²⁺ influx induced by delivering the train-stimulus in both cells (stim, *inset*). This inhibition of junctional communication lasts for at least 15 min. *Inset* shows the voltage step to provoke junctional current. Scale bars apply to both traces. **B:** when the standard saline in the pipettes is replaced with one containing 40 mM EGTA, elevation of intracellular Ca²⁺ with the train-stimulus fails to inhibit junctional current. Scale bars apply to both traces. **C:** average data comparing the junctional current after Ca²⁺ influx in pairs dialyzed with a high (40 mM or 20 mM) vs. standard (5 mM) concentration of EGTA. The difference in the Ca²⁺-induced decrease in junctional current between standard EGTA and 40 mM EGTA is significant ($F_{2,18} = 7.43$, $P < 0.02$, ANOVA; Dunnett multiple-comparisons test).



junctional current to the train-stimulus; however, this was not significantly different from control (Fig. 5C).

CaM-kinase appears to be involved in Ca²⁺-induced uncoupling. A previous description of bag cell neurons showed that CaM-kinase was activated during the afterdischarge (DeRiemer et al. 1984). Moreover, the prolonged time course of the Ca²⁺-induced inhibition of bag cell neuron gap junctions suggests a biochemical intermediate. To determine whether CaM-kinase participates in the regulation of bag cell neuron electrical synapses, we initially employed KN-62, an isoquinolinesulfonamide-derived CaM-kinase II antagonist that is effective in *Aplysia* (Hung and Magoski 2007; Nakanishi et al. 1997; Tokumitsu et al. 1990). Pairs were treated for 15 min prior to recording in DMSO or KN-62 and voltage-clamped for 30 min, and then junctional current was elicited (Fig. 6A, inset). As expected, the train-stimulus in DMSO (vehicle)-treated neurons ($n = 9$) produced an $\sim 20\%$ decrease in junctional current (Fig. 6A). A similar inhibition of junctional current was observed when neurons were stimulated in 10 μM KN-62 ($n = 5$; Fig. 6D); however, 50 μM KN-62 ($n = 6$) prevented the uncoupling effect of Ca²⁺ influx (Fig. 6B), which was statistically different from control (Fig. 6D). As further confirmation, KN-93, a methoxybenzenesulfonamide that also inhibits CaM-kinase (Sumi et al. 1991), along with its structurally related but inactive analog, KN-92, were used. A 15-min incubation with 10 μM KN-93 ($n = 5$) precluded the ability of Ca²⁺ to lower coupling, with only an $\sim 4\%$ drop (Fig. 6C). This was not the case for 10 μM KN-92, which failed to impede suppression of the electrical synapse by stimulation; the difference in the Ca²⁺-induced decrease in junctional current between KN-92 and KN-93 was significant (Fig. 6E).

A PKC activator reduces junctional current. Shortly after the onset of the afterdischarge, PKC activity was shown to be upregulated and stayed elevated throughout (Conn et al. 1989a; Wayne et al. 1999). Because PKC has been established as a modulator of electrical coupling in various cells (Lampe et al. 2000; Saez et al. 1990), the effect of the phorbol ester PMA, a potent and selective PKC activator in bag cell neurons (Cast-

agna et al. 1982; Sossin et al. 1993), was tested on junctional current (Fig. 7A, inset). Given that Ca²⁺ influx and PKC upregulation would occur at similar times in the intact cluster (Fisher et al. 1994; Wayne et al. 1999), we also subjected these preparations to the train-stimulus. In controls, the addition of DMSO (the vehicle) to pairs of coupled neurons ($n = 4$) did not appreciably alter the junctional current (Fig. 7A, center) compared with the initial response (Fig. 7A, left). Subsequent delivery of the train-stimulus to these cells resulted in an $\sim 25\%$ inhibition (Fig. 7A, right). In contrast, introducing 100 nM PMA to electrically coupled neurons ($n = 13$) decreased the junctional current by $\sim 15\%$ (Fig. 7B, center vs. left). Moreover, the combination of PMA and the train-stimulus was more effective at lowering electrical coupling than PMA alone and caused an $\sim 35\%$ decrease in junctional current (Fig. 7B, right). Summary data showed a significant difference in junctional current between control pairs and those treated with PMA (Fig. 7C). Also, the PMA-induced uncoupling was additive with Ca²⁺ influx, where stimulation plus PKC activation presented a significantly greater inhibition than PKC activation alone or stimulation alone (Fig. 7C).

Elevated intracellular Ca²⁺ decreases amplitude and time course of electrotonic transmission. Electrical coupling mediates synchronous action potential firing of bag cell neurons throughout the afterdischarge (Blankenship and Haskins 1979; Brown et al. 1989). We sought to test the impact of Ca²⁺ influx on the ETP evoked by action potentials in the presynaptic neuron. Action potential-like waveforms were generated in one neuron under voltage clamp, and the ETP was recorded in the second cell under current clamp. Idealized action potentials, based on spikes recorded during prior work from our lab, were favored over actual spikes, to avoid changes to the waveform that can occur after repetitive stimulation and Ca²⁺ influx (Acosta-Urquidí and Dudek 1981; Hung and Magoski 2007). In control pairs ($n = 5$), a series of voltage ramps from -60 mV, mimicking the action potential, was delivered to the presynaptic neuron under voltage clamp (Fig. 8A, bottom), which in turn elicited a postsynaptic ETP in the coupled partner

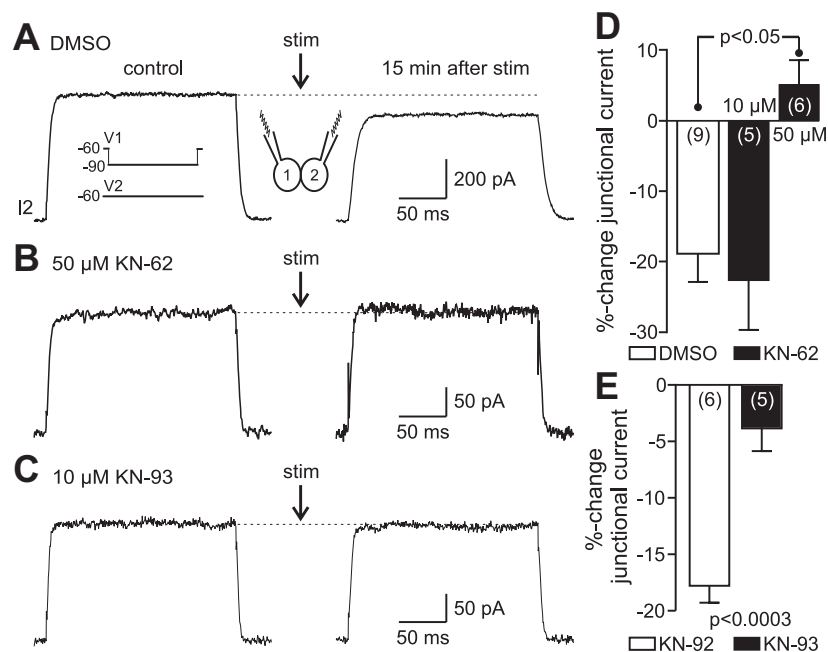


Fig. 6. Inhibition of calmodulin (CaM)-kinase prevents the Ca²⁺-dependent decrease in electrical coupling. *A*: in a pair treated with DMSO and then dialyzed under voltage clamp at -60 mV for 30 min, elevating intracellular Ca²⁺ with the train-stimulus to both neurons (inset) causes a decrease in junctional current (I₂) for up to 15 min. Inset provides the voltage protocol to elicit junctional current. Scale bars apply to both traces. *B* and *C*: a 15-min exposure to 50 μM of KN-62, a CaM-kinase antagonist, averts the uncoupling effect of elevated intracellular Ca²⁺, and, similarly, 20 min of 10 μM KN-93, a different blocker of CaM-kinase, also renders Ca²⁺ influx incapable of attenuating junctional current. Scale bars apply to both traces in *B* and *C*, respectively. *D*: % change in junctional current after stimulation in KN-62 vs. DMSO. A 50 μM , but not 10 μM , concentration of KN-62 significantly inhibits the uncoupling effect of Ca²⁺ ($F_{2,12} = 7.87$, $P < 0.01$, ANOVA; Dunnett multiple-comparisons test). *E*: summary data for the effect of KN-93 and its inactive analog, KN-92, on Ca²⁺ entry-induced % change in junctional current. While 10 μM KN-92 does not impact uncoupling, the presence of 10 μM KN-93 eliminates any Ca²⁺-evoked alteration. The change in KN-93 is significantly less than in KN-92 (unpaired Student's *t*-test).

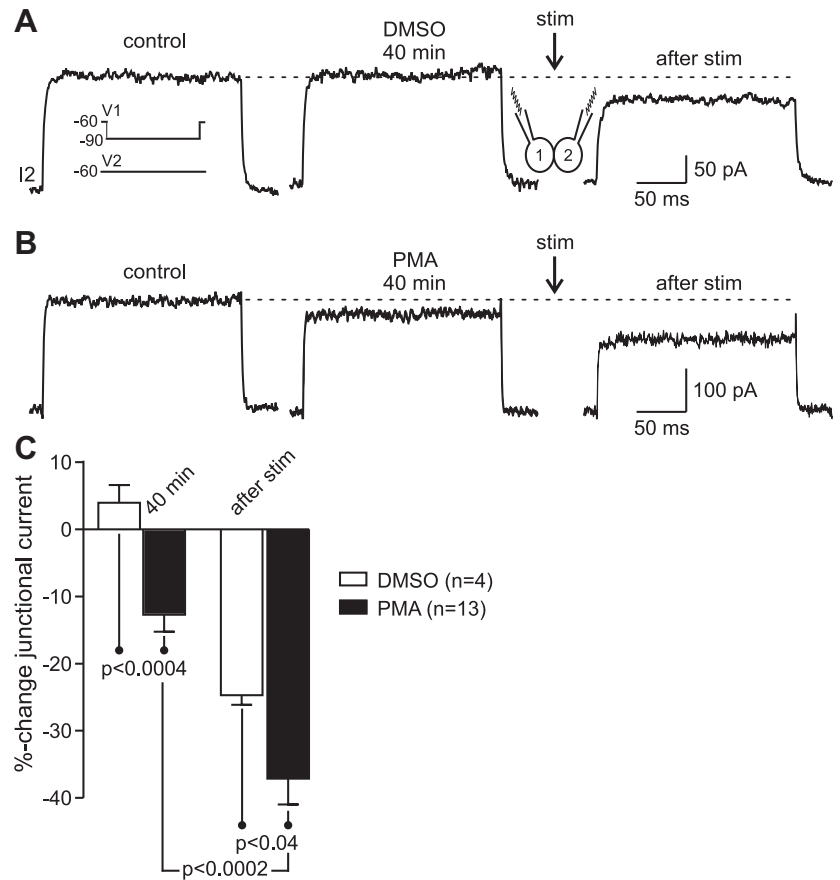


Fig. 7. A protein kinase C (PKC) activator inhibits gap junctions and interacts with Ca²⁺ influx. **A**: exposure of a control pair of coupled bag cell neurons to DMSO for 40 min (*left*) does not cause an appreciable change in junctional current (I₂) (*center*). Ca²⁺ influx (stim; diagram represents paired neurons with stimulation to both pipettes) produced by the train-stimulus reduces the junctional current (*right*). *Inset* depicts the command voltage to evoke junctional current in neuron 2 (I₂). Scale bars apply to all traces. **B**: introduction of 100 nM PKC activator phorbol 12-myristate 13-acetate (PMA) modestly suppresses the junctional current, while subsequent elevation of intracellular Ca²⁺ in these neurons inhibits the gap junction to an even greater extent. Scale bars apply to all traces. **C**: group data comparing mean % change in junctional current following DMSO or PMA. The difference between DMSO and neurons in which PKC is triggered is significant (unpaired Student's *t*-test). The inhibitory effect of Ca²⁺ influx is also significantly larger when PMA is present compared with just Ca²⁺ entry (unpaired Student's *t*-test). Moreover, stimulation + PMA is has a significantly greater impact than PMA alone (unpaired Student's *t*-test).

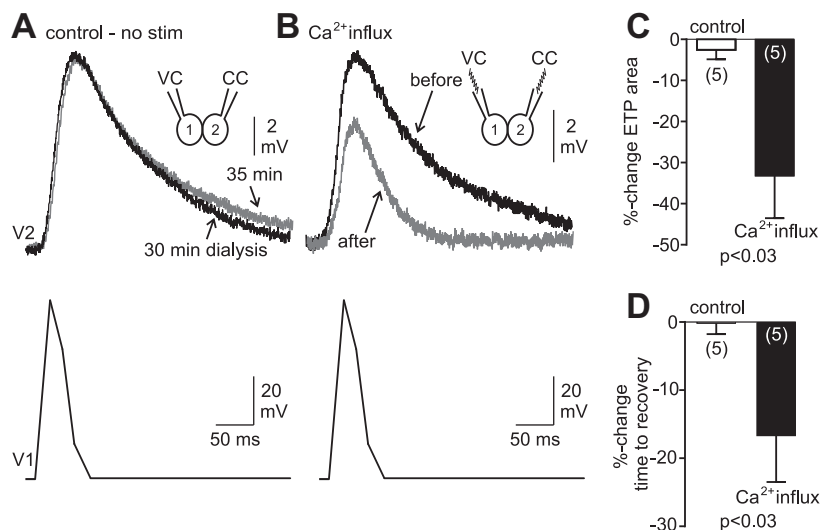
current-clamped to -60 mV with bias current (Fig. 8A, *top*). The control ETP lasted three to four times longer than the presynaptic waveform and did not change over time (Fig. 8A, *top*). However, when both neurons were given the train-stimulus ($n = 5$) under voltage clamp to increase Ca²⁺, the same action potential-like waveform (Fig. 8B, *bottom*) produced a smaller and faster ETP compared with the initial ETP (Fig. 8B, *top*). Both the area of the ETP as well as the time required to recover from the peak response to steady-state showed a significant decrease in stimulated vs. unstimulated control (Fig. 8, C and D). Additionally, for the stimulated pairs

the input resistance was measured in the postsynaptic cell both before and after the train-stimulus, by delivering a -250 pA, 1,500-ms hyperpolarization current step from -60 mV. Postsynaptic input resistance did not change appreciably after Ca²⁺ entry ($2.2 \pm 15.6\%$).

DISCUSSION

Cytosolic Ca²⁺ is vital to the regulation of fundamental processes such as channel gating, excitability, and secretion (Hille 2001). Elevated intracellular Ca²⁺ decreases electrical

Fig. 8. Elevated intracellular Ca²⁺ reduces the size and time course of the ETP. **A**: simultaneous voltage- and current-clamp recording from a pair of electrically coupled neurons. From a holding potential of -60 mV, an idealized action potential waveform (*bottom*) (composed of 4 ramps: to $+10$ mV over 20 ms, -10 mV over 15 ms, -45 mV over 15 ms, and then back to -60 mV over 20 ms) to neuron 1 (V1) delivered in voltage clamp elicits an ETP in neuron 2 (V2) (*top*, black trace, 30-min dialysis) recorded in current clamp. The amplitude of the ETP does not appreciably change over time (*top*, gray trace, 35 min). *Inset*: neuron 1 is voltage clamped (VC) while neuron 2 is recorded under current clamp (CC). Time base applies to all traces. **B**: the action potential waveform in neuron 1 (*bottom*) produces an ETP in neuron 2 (*top*, black trace, before). Simultaneously delivering to both cells the train-stimulus (*inset*; 5 Hz, 1 min then 1 Hz, 5 min) causes a smaller ETP that recovers faster (*top*, gray trace, after); recorded immediately after the train-stimulus. Time base applies to all traces. **C** and **D**: summary graphs comparing mean change in ETP area (**C**) and time to recovery (**D**) in neuron 2 evoked by the waveform in neuron 1 show both parameters are significantly less after Ca²⁺ influx compared with control conditions of no stimulation (unpaired Student's *t*-test).



coupling in many excitable and nonexcitable cells (Peracchia 2004; Rohr 2004; Saez et al. 1989; Sohl and Willecke 2004; Spray and Bennett 1985). For neurons, voltage-gated Ca²⁺ channels are the primary means to increase Ca²⁺ (Catterall and Few 2008). In bag cell neurons, delivery of the 5-Hz, 1-min then 1-Hz, 5-min stimulus mimics the fast and early slow phases of the afterdischarge, leading to an immediate and prominent Ca²⁺ influx. The Ca²⁺ rise inhibits electrical transmission between pairs of cultured bag cell neurons. During the afterdischarge in the intact cluster, the fast phase sees Ca²⁺ change from a resting level of ~300 nM to a peak of ~800 nM, followed by a slow-phase plateau of ~450 nM (Fisher et al. 1994). For the present study, the alterations in cultured bag cell neuron intracellular Ca²⁺, as monitored with fura, would approximate those seen in situ. Thus it would be reasonable to suggest that increasing Ca²⁺ by hundreds of nanomolar would be sufficient to close gap junctions.

Stimulation in Ca²⁺-free medium is ineffective at inhibiting the electrical synapse, implicating Ca²⁺ entry as the cause of uncoupling. This is consistent with Chanson et al. (1999), who showed that a Ca²⁺-induced reduction in junctional current between acinar cells is occluded by removing external Ca²⁺. Furthermore, high-EGTA intracellular saline prevents bag cell neuron uncoupling, supporting the role of intracellular Ca²⁺ in electrical synapse suppression. The Ca²⁺-mediated decrease in junctional conductance between hepatoma cells is also attenuated by EGTA (Lazrak and Peracchia 1993) and another Ca²⁺ buffer, BAPTA (Lazrak et al. 1994). There are contradictory findings as to whether Ca²⁺ rising in only one cell will curb electrical transmission: In coupled rat hepatocytes, imaging shows that injection of Ca²⁺ in one cell increases Ca²⁺ in the adjacent cell (Saez et al. 1989). Conversely, Rose and Loewenstein (1976) found that Ca²⁺ injected into a single *Chironomus* salivary gland cell not only fails to cause uncoupling but also does not diffuse to a neighboring cell. This parallels our finding that a train-stimulus to both bag cell neurons, rather than only one, is needed to chronically inhibit junctional current. In those pairs where we stimulated just one neuron, it is likely that Ca²⁺ reaches the junctional region but induces only partial uncoupling, perhaps because of a failure of Ca²⁺ to pass through the junction, because the Ca²⁺ does not fully activate the necessary transduction pathway(s), or because full closure of the gap junction requires both participating innexons to enter a shut state.

In bag cell neurons, intracellular stores contribute to Ca²⁺ dynamics, particularly during the slow phase of the afterdischarge (Fisher et al. 1994; Geiger and Magoski 2008). On entry, Ca²⁺ is taken up by the mitochondria through the Ca²⁺ uniporter and then released through cation exchangers to stimulate ryanodine receptors on the endoplasmic reticulum and release further Ca²⁺ (Geiger and Magoski 2008). When we eliminate the ability of mitochondria to clear intracellular Ca²⁺ with the protonophore FCCP, it causes a substantial and concentration-dependent decrease in the bag cell neuron junctional current. However, endoplasmic reticulum Ca²⁺ depletion by the pump inhibitor CPA does not impact coupling, nor does a high concentration of ryanodine alter the reduction in the electrical synapse brought about by stimulation. This is consistent with our prior work showing that mitochondrial, but not endoplasmic reticulum, Ca²⁺ has preferential access to both gate a plasma membrane cation channel and evoke neuropeptide secretion (Hickey et al. 2010,

2013). Although FCCP impacts the mitochondria, it is most probable that the drop in coupling is from Ca²⁺ rather than a change in cell health. This is based on the FCCP-induced current we reported previously not being due to Ca²⁺-activated proteases, reactive oxygen species, or a general disruption of mitochondrial function (Hickey et al. 2010). In *Chironomus* salivary gland cyanide, which prevents oxidative metabolism and frees mitochondrial Ca²⁺ (Carafoli 1967), suppresses gap junctions (Rose and Loewenstein 1975). Conversely, blocking the endoplasmic reticulum Ca²⁺ pump with thapsigargin (Thastrup et al. 1990) reduces coupling between pancreatic acinar cells (Chanson et al. 1999).

Others have suggested that Ca²⁺-dependent reductions in coupling are a secondary effect of Ca²⁺ acidifying the cytoplasm or Ca²⁺ synergizing with acidosis (Lazrak and Peracchia 1993). For example, Ca²⁺ or H⁺ alone does not block coupling between rat myocardial cells, but coupling decreases when acidosis accompanies Ca²⁺ (Burt 1987). Also, CO₂-mediated cytosolic acidification lowers electrical coupling in the presence of normal Ca²⁺, whereas removing extracellular Ca²⁺ prevents this effect (White et al. 1990). Conversely, a drop in junctional communication between crayfish axons is related to a Ca²⁺ increase rather than low pH (Peracchia 1990). For bag cell neurons, there is evidence to rule out H⁺ as a factor in Ca²⁺-induced uncoupling: First, substantially elevating Ca²⁺ in these cells by pharmacological activation of a store-operated influx pathway does not change intracellular pH (Knox et al. 2004). Second, in the present study, we included HEPES in the intracellular saline, which would work to halt any Ca²⁺-evoked change in pH. Third, our intracellular dialysis with the Ca²⁺ chelator EGTA eliminates the effect of Ca²⁺. Fourth, we show that CaM-kinase blockers prevent uncoupling.

Ca²⁺ might not always impact gap junctions directly but rather via a cytoplasmic intermediate. CaM is a ubiquitous Ca²⁺-binding protein that can bind gap junctions (Van Eldik et al. 1985) and is well-established as an ion channel regulator (Levitan 1999). Typically, CaM inhibits gap junctions, as first suggested in *Xenopus* oocytes (Peracchia et al. 1983) and crayfish axons (Peracchia 1987) as well as other vertebrate (Toyama et al. 1994) and invertebrate (Arellano et al. 1988) systems. CaM can also activate CaM-kinase, which phosphorylates a wide variety of proteins (Coultrap and Bayer 2012; Wayman et al. 2008). Interestingly, CaM-kinase has been largely found to enhance junctional conductance, such as in goldfish Mauthner neurons (Pereda et al. 1998), mouse astrocytes (De Pina-Benabou et al. 2001), and neuroblasma cells expressing rat Cx36 (Del Corso et al. 2012). We show here that CaM-kinase may have a role in Ca²⁺-evoked inhibition of the bag cell neuron electrical synapse, based on the CaM-kinase antagonists KN-62 and KN-93 both preventing the uncoupling effect of Ca²⁺. DeRiemer et al. (1984, 1985) found that *Aplysia* CaM-kinase is homologous to that in mammals and may mediate the long-lasting effect of intracellular Ca²⁺ entry during the afterdischarge. CaM blockers inhibit *Aplysia* CaM-kinase in a biochemical assay and the ability of the bag cell neurons to fire an afterdischarge. In cultured bag cell neurons, KN-62 also attenuates a prolonged depolarization and cation channel activation evoked by Ca²⁺ influx (Hung and Magoski 2007).

Uncoupling by Ca²⁺ is associated with a decrease in junctional thickness and a reduction in gap junction pore diameter (Bernardini and Peracchia 1981; Peracchia and Dulhunty

1976). There is also evidence for so-called slow gating of gap junctions, where Ca²⁺-CaM promotes more lengthy transitions between open and closed states, as well as a greater time in residual conductance states (Peracchia 2004). These changes may be due to phosphorylation (Moreno et al. 1994), and potential phosphorylation sites for various kinases have been identified in many connexins (Cruciani and Mikalsen 2002; Giepmans 2004; Laird 2005; Solan and Lampe 2005) and some innexins (Bauer et al. 2005; Potenza et al. 2002). Phosphorylation can change the unitary conductance or open probability of gap junction channels (Moreno and Lau 2007). CaM-kinase phosphorylates Cx32 on Ser residues (Saez et al. 1990) and Cx36 specifically on Ser110 and Thr111 (Alev et al. 2008). We propose that a combination of Ca²⁺ and protein phosphorylation regulates bag cell neuron intercellular communication. The average change in junctional conductance following voltage-gated Ca²⁺ influx for all control pairs in the present study was an ~25% decrease (10.5 ± 1.8 nS before vs. 7.9 ± 0.6 nS after stimulation; $n = 38$, $P < 0.0001$, Wilcoxon matched-pairs signed-ranks test). This may serve to elevate excitability by increasing system input resistance in the intact cluster. For instance, neurons could become more responsive to the cholinergic synaptic input that drives the start of the afterdischarge or the cation and persistent Ca²⁺ currents that maintain the depolarization (Hung and Magoski 2007; Magoski et al. 2000; Tam et al. 2009, 2011; White and Magoski 2012).

To examine the impact of reduced coupling at the network level, we modeled 100 Hodgkin-Huxley-type neurons serially connected in a row by voltage-independent gap junctions [models modified from Hodgkin and Huxley (1952), Izhikevich (2007), and Ermentrout et al. (2004); see *Model development* for details]. The model also included a persistent Ca²⁺ current (Carlin et al. 2000) to make the neurons fire tonically in a manner qualitatively similar to the bag cell neurons. Brown and Mayeri (1989) envisaged action potentials spatially spreading from neurons driven to fire in the center of the cluster at the onset of afterdischarge. Hence, model cells 35–64 received excitatory, ionotropic-type cholinergic synaptic input. The activity of all neurons was monitored for 5 s, starting with brief periodic synaptic stimulation (100 ms, 20 Hz). We initially set

the junctional conductance (0.14 mS/cm²) at just under half of the membrane conductance (0.3 mS/cm²), as per our prior experimental findings (Dargaei et al. 2014). In this case, stimulation caused 65 of 100 neurons to spike, with excitation spreading from those receiving input to only some of the neurons down the line (Fig. 9A). However, when the junctional conductance was lowered by 25% to 0.105 mS/cm², mimicking Ca²⁺-dependent inhibition, nearly all 100 neurons fired (Fig.

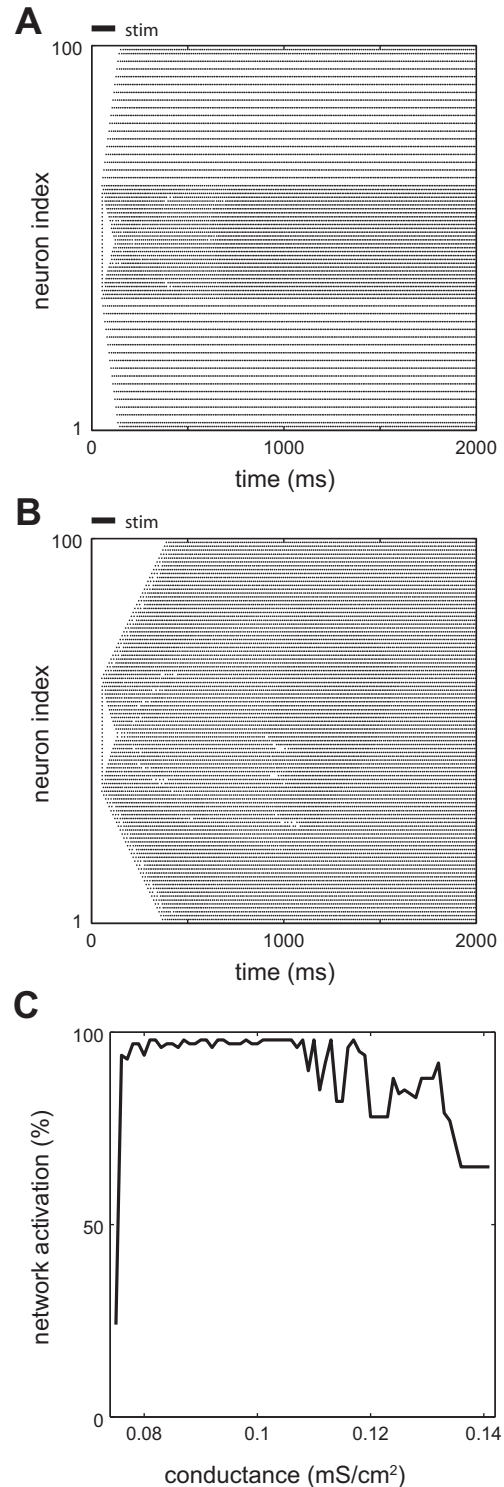


Fig. 9. Reducing junctional conductance in a model of electrically coupled neurons improves recruitment. *A*: raster diagram denoting spiking of all 100 model neurons, serially connected by gap junctions with a conductance of 0.14 mS/cm². During the initial 100 ms of the trial, neurons 35–64 are given excitatory chemical synaptic input (at bar, stim). Although all of these cells fire action potentials for nearly the entire time, the spread of excitation to other neurons is less robust, with essentially every other cell spiking. In addition, excitation proceeds rapidly from the center and reaches a maximum of 65 of 100 neurons firing just after the end of the stimulus. Note that although the trials are 5 s long, both *A* and *B* are truncated at 2 s to better display the temporal aspects of recruitment. Neuron index on the ordinate refers to each individual cell. *B*: when junctional conductance is reduced by 25% to 0.105 mS/cm², as per the effect of Ca²⁺ influx on the electrical synapse, exciting the same central group of neurons (at bar, stim) eventually recruits almost all of the remaining cells to spike. However, this is delayed and achieves a maximum of 98 of 100 neurons only several hundred milliseconds after chemical input has ceased. *C*: the percentage of neurons firing vs. junctional conductance magnitude taken over the final 100 ms of each trial. The strengths of the electrical synapses are increased in 0.001 mS/cm² increments from 0.075 to 0.14 mS/cm². When the gap junctions are weak (<0.076 mS/cm²), no additional neurons are recruited, and just those cells given stimulation fire. However, between 0.076 and 0.11 mS/cm² more or less every neuron spikes. Beyond 0.11 mS/cm², recruitment begins to vary and becomes markedly poorer as the extent of coupling approaches 0.14 mS/cm².

9B). When comparing the raster plots of action potential firing in all neurons for the two conditions, the lower junctional conductance showed more gradual, albeit more effective recruitment. Furthermore, recruitment varied when junctional conductance was between 0.14 and 0.11 mS/cm², sometimes approaching all neurons while in other instances only ~70 neurons, with the performance being worse closer to 0.14 mS/cm² (Fig. 9C). This variability was due to junctional current being unable to recruit every neuron, on account of it leaking into adjacent cells. Nevertheless, when the junctional conductance was around 0.1 mS/cm², the performance of the network stabilized and all neurons consistently spiked. Not surprisingly, at low junctional conductances (<0.076 mS/cm²) there was no spatial spread of excitation and only neurons receiving synaptic input fired.

During the slow phase of the afterdischarge, PKC turns on and stays elevated (Conn et al. 1989a; Wayne et al. 1999). PKC activation enhances voltage-gated Ca²⁺ current and increases the overall amount of Ca²⁺ during the afterdischarge (DeRiemer et al. 1985). Application of the phorbol ester PMA activates *Aplysia* PKC, as seen in both biochemical assays of nervous system ganglia and bag cell neurons in the intact cluster or primary culture (DeRiemer et al. 1985; Sossin et al. 1993; Sossin and Schwartz 1992; Tam et al. 2011). The ability of PKC to close gap junctions has been shown in a number of cell types (Cruciani et al. 2001; Lampe et al. 2000; Spray and Bennett 1985). In our study, PMA inhibited electrical coupling, supporting the involvement of PKC in the regulation of bag cell neuron gap junctions. Inhibition was even greater when PMA-treated cells were given the train-stimulus to increase intracellular Ca²⁺. Accordingly, as Ca²⁺ falls somewhat during the slow phase, PKC could maintain inhibition by having a cumulative effect with the remaining Ca²⁺.

A reduction in coupling may also, somewhat paradoxically, promote synchrony during the afterdischarge. Ca²⁺ influx decreases the amplitude and time course of the ETP produced by a presynaptic action potential-like waveform. Typical of most gap junctions, the bag cell neuron electrical synapse is a low-pass filter (Dargaei et al. 2014), which sustains the ETP well beyond the time course of the presynaptic spike. A modest decrease in junctional conductance may improve synchrony by preventing lengthy ETPs and out-of-phase postsynaptic action potentials. The fact that postsynaptic input resistance did not change after Ca²⁺ entry suggests that the altered ETP is due to a drop in coupling. However, it is worth noting that our prior work on single cells showed an ~30% fall in input resistance (or ~45% increase in membrane conductance) after stimulation, on account of the opening of a calcium-activated, voltage-independent cation channel (Hickey et al. 2010; Hung and Magoski 2007). Thus the lack of input resistance change we observed in the present study may be due to a simultaneous loss of some junctional conductance and gain of some membrane conductance.

It is unlikely that bag cell neuron synchrony would be impaired by the intermediate suppression of electrical transmission we observe here, as even weakly coupled networks synchronize (Gibson et al. 1999; Landisman et al. 2002; Traub et al. 2001). Tetanic stimulation in the thalamus also inhibits electrical synapses between reticular neurons for periods similar to what we observe in *Aplysia* (Landisman and Connors 2005). In acinar pancreatic cells, Ca²⁺-induced uncoupling

leads to enhanced hormone secretion (Chanson et al. 1998, 1999). Furthermore, an increased ETP between electrically coupled neuroendocrine cells of cockroach is correlated to reduced juvenile hormone secretion (Lococo et al. 1986). Synchrony may be essential for ELH secretion from bag cell neurons, and a modest decrease in electrotonic transmission could help to ensure in-phase spiking and consistently timed hormone release necessary for reproduction.

ACKNOWLEDGMENTS

The authors thank H. M. Hodgson for technical assistance and N. M. Magoski for critical evaluation of previous drafts of the manuscript.

GRANTS

Z. Dargaei held a Queen's Graduate Award. This work was supported by Natural Sciences and Engineering Research Council of Canada discovery grants to both G. Blohm and N. S. Magoski as well as Canada Foundation for Innovation and Ontario Research Fund grants to G. Blohm.

DISCLOSURES

No conflicts of interest, financial or otherwise, are declared by the author(s).

AUTHOR CONTRIBUTIONS

Author contributions: Z.D., D.S., and C.J.G. performed experiments; Z.D., D.S., C.J.G., and N.S.M. analyzed data; Z.D., D.S., and N.S.M. interpreted results of experiments; Z.D., D.S., C.J.G., and N.S.M. prepared figures; Z.D. drafted manuscript; Z.D., D.S., C.J.G., G.B., and N.S.M. approved final version of manuscript; G.B. and N.S.M. conception and design of research; G.B. and N.S.M. edited and revised manuscript.

REFERENCES

- Acosta-Urquidí J, Dudek FE. Soma spike of neuroendocrine bag cells of *Aplysia californica*. *J Neurobiol* 12: 367–378, 1981.
- Alev C, Urschel S, Sonntag S, Zoidl G, Fort AG, Höher T, Matsubara M, Willecke K, Spray DC, Dermietzel R. The neuronal connexin36 interacts with and is phosphorylated by CaMKII in a way similar to CaMKII interaction with glutamate receptors. *Proc Natl Acad Sci USA* 105: 20964–20969, 2008.
- Arellano RO, Ramón F, Rivera A, Zampighi GA. Lowering of pH does not directly affect the junctional resistance of crayfish lateral axons. *J Membr Biol* 94: 293–299, 1986.
- Bauer R, Löer B, Ostrowski K, Martini J, Weimbs A, Lechner H, Hoch M. Intercellular communication: the *Drosophila* innexin multiprotein family of gap junction proteins. *Chem Biol* 12: 515–526, 2005.
- Baux G, Simonneau M, Tauc L, Segundo JP. Uncoupling of electrotonic synapses by calcium. *Proc Natl Acad Sci USA* 75: 4577–4581, 1978.
- Bennett MV, Zukin RS. Electrical coupling and neuronal synchronization in the mammalian brain. *Neuron* 41: 495–511, 2004.
- Bernardini G, Peracchia C. Gap junction crystallization in lens fibers after an increase in cell calcium. *Invest Ophthalmol Vis Sci* 21: 291–299, 1981.
- Blankenship JE, Haskins JT. Electrotonic coupling among neuroendocrine cells in *Aplysia*. *J Neurophysiol* 42: 347–355, 1979.
- Brown RO, Mayeri E. Positive feedback by autoexcitatory neuropeptides in neuroendocrine bag cells of *Aplysia*. *J Neurosci* 9: 1443–1451, 1989.
- Brown RO, Pulst SM, Mayeri E. Neuroendocrine bag cells of *Aplysia* are activated by bag cell peptide-containing neurons in the pleural ganglion. *J Neurophysiol* 61: 1142–1152, 1989.
- Burr GR, Mitchell CK, Keflemariam YJ, Heidelberger R, O'Brien J. Calcium-dependent binding of calmodulin to neuronal gap junction proteins. *Biochem Biophys Res Commun* 335: 1191–1198, 2005.
- Burt JM. Block of intercellular communication: interaction of intracellular H⁺ and Ca²⁺. *Am J Physiol Cell Physiol* 253: C607–C612, 1987.
- Carafoli E. In vivo effect of uncoupling agents on the incorporation of calcium and strontium into mitochondria and other subcellular fractions of rat liver. *J Gen Physiol* 50: 1849–1864, 1967.

- Carlin KP, Jiang Z, Brownstone RM.** Characterization of calcium currents in functionally mature mouse spinal motoneurons. *Eur J Neurosci* 12: 1624–1634, 2000.
- Castagna M, Takai Y, Kaibuchi K, Sano K, Kikkawa U, Nishizuka Y.** Direct activation of calcium-activated, phospholipid-dependent protein kinase by tumor-promoting phorbol esters. *J Biol Chem* 257: 7847–7851, 1982.
- Catterall WA, Few AP.** Calcium channel regulation and presynaptic plasticity. *Neuron* 59: 882–901, 2008.
- Chanson M, Fanjul M, Bosco D, Nelles E, Suter S, Willecke K, Meda P.** Enhanced secretion of amylase from exocrine pancreas of connexin32-deficient mice. *J Cell Biol* 141: 1267–1275, 1998.
- Chanson M, Mollard P, Meda P, Suter S, Jongasma HJ.** Modulation of pancreatic acinar cell to cell coupling during ACh-evoked changes in cytosolic Ca²⁺. *J Biol Chem* 274: 282–287, 1999.
- Conn PJ, Strong JA, Azhderian EM, Nairn AC, Greengard P, Kaczmarek LK.** Protein kinase inhibitors selectively block phorbol ester- or forskolin-induced changes in excitability of *Aplysia* neurons. *J Neurosci* 9: 473–479, 1989a.
- Conn PJ, Strong JA, Kaczmarek LK.** Inhibitors of protein kinase C prevent enhancement of calcium current and action potentials in peptidergic neurons of *Aplysia*. *J Neurosci* 9: 480–487, 1989b.
- Coultrap SJ, Bayer KU.** CaMKII regulation in information processing and storage. *Trends Neurosci* 35: 607–618, 2012.
- Cruciani V, Husøy T, Mikalsen S.** Pharmacological evidence for system-dependent involvement of protein kinase C isoenzymes in phorbol ester-suppressed gap junctional communication. *Exp Cell Res* 268: 150–161, 2001.
- Cruciani V, Mikalsen S.** Connexins, gap junctional intercellular communication and kinases. *Biol Cell* 94: 433–443, 2002.
- Dahl G, Isenberg G.** Decoupling of heart muscle cells: correlation with increased cytoplasmic calcium activity and with changes of nexus ultrastructure. *J Membr Biol* 53: 63–75, 1980.
- Dargaei Z, Colmers PL, Hodgson HM, Magoski NS.** Electrical coupling between *Aplysia* bag cell neurons: characterization and role in synchronous firing. *J Neurophysiol* (September 3, 2014). doi:10.1152/jn.00494.2014.
- De Mello WC.** Effect of intracellular injection of calcium and strontium on cell communication in heart. *J Physiol* 250: 231–245, 1975.
- De Pina-Benabou MH, Srinivas M, Spray DC, Scemes E.** Calmodulin kinase pathway mediates the K⁺-induced increase in gap junctional communication between mouse spinal cord astrocytes. *J Neurosci* 21: 6635–6643, 2001.
- Del Corso C, Iglesias R, Zoidl G, Dermietzel R, Spray DC.** Calmodulin dependent protein kinase increases conductance at gap junctions formed by the neuronal gap junction protein connexin36. *Brain Res* 1487: 69–77, 2012.
- DeRiemer SA, Kaczmarek LK, Lai Y, McGuinness TL, Greengard P.** Calcium/calmodulin-dependent protein phosphorylation in the nervous system of *Aplysia*. *J Neurosci* 4: 1618–1625, 1984.
- DeRiemer SA, Strong JA, Albert KA, Greengard P, Kaczmarek LK.** Enhancement of calcium current in *Aplysia* neurons by phorbol ester and protein kinase C. *Nature* 313: 313–316, 1985.
- Dermietzel R, Spray DC.** Gap junctions in the brain: where, what type, how many and why? *Trends Neurosci* 16: 186–192, 1993.
- Ermentrout B, Wang J, Flores J, Gelperin A.** Model for transition from waves to synchrony in the olfactory lobe of *Limax*. *J Comput Neurosci* 17: 365–383, 2004.
- Fisher TE, Levy S, Kaczmarek LK.** Transient changes in intracellular calcium associated with a prolonged increase in excitability in neurons of *Aplysia californica*. *J Neurophysiol* 71: 1254–1257, 1994.
- Geiger JE, Magoski NS.** Ca²⁺-induced Ca²⁺ release in *Aplysia* bag cell neurons requires interaction between mitochondrial and endoplasmic reticulum stores. *J Neurophysiol* 100: 24–37, 2008.
- Gibson JR, Beierlein M, Connors BW.** Two networks of electrically coupled inhibitory neurons in neocortex. *Nature* 402: 75–79, 1999.
- Giepmans BN.** Gap junctions and connexin-interacting proteins. *Cardiovasc Res* 62: 233–245, 2004.
- Groten CJ, Rebane JT, Blohm G, Magoski NS.** Separate Ca²⁺ sources are buffered by distinct Ca²⁺ handling systems in *Aplysia* neuroendocrine cells. *J Neurosci* 33: 6476–6491, 2013.
- Grynkiewicz G, Poenie M, Tsien RY.** A new generation of Ca²⁺ indicators with greatly improved fluorescence properties. *J Biol Chem* 260: 3440–3450, 1985.
- Heytler P, Prichard W.** A new class of uncoupling agents—carbonyl cyanide phenylhydrazones. *Biochem Biophys Res Commun* 7: 272–275, 1962.
- Hickey CM, Geiger JE, Groten CJ, Magoski NS.** Mitochondrial Ca²⁺ activates a cation current in *Aplysia* bag cell neurons. *J Neurophysiol* 103: 1543–1556, 2010.
- Hickey CM, Groten CJ, Sham L, Carter CJ, Magoski NS.** Voltage-gated Ca²⁺ influx and mitochondrial Ca²⁺ initiate secretion from *Aplysia* neuroendocrine cells. *Neuroscience* 250: 755–772, 2013.
- Hille B.** *Ion Channels of Excitable Membranes*. Sunderland, MA: Sinauer, 2001, chapt. 16, p. 504–536.
- Hodgkin AL, Huxley AF.** A quantitative description of membrane current and its application to conduction and excitation in nerve. *J Physiol* 10: 500–544, 1952.
- Hung AY, Magoski NS.** Activity-dependent initiation of a prolonged depolarization in *Aplysia* bag cell neurons: role for a cation channel. *J Neurophysiol* 97: 2465–2479, 2007.
- Izhikevich EM.** *Dynamical Systems in Neuroscience*. Cambridge, MA: MIT Press, 2007.
- Kachoei BA, Knox RJ, Uthusa D, Levy S, Kaczmarek LK, Magoski NS.** A store-operated Ca²⁺ influx pathway in the bag cell neurons of *Aplysia*. *J Neurophysiol* 96: 2688–2698, 2006.
- Kaczmarek LK, Finbow M, Revel JP, Strumwasser F.** The morphology and coupling of *Aplysia* bag cells within the abdominal ganglion and in cell culture. *J Neurobiol* 10: 535–550, 1979.
- Kaczmarek LK, Jennings K, Strumwasser F.** Neurotransmitter modulation, phosphodiesterase inhibitor effects, and cyclic AMP correlates of afterdischarge in peptidergic neurites. *Proc Natl Acad Sci USA* 75: 5200–5204, 1978.
- Kaczmarek LK, Jennings K, Strumwasser F.** An early sodium and a late calcium phase in the afterdischarge of peptide-secreting neurons of *Aplysia*. *Brain Res* 238: 105–115, 1982.
- Knox RJ, Magoski NS, Wing D, Barbee SJ, Kaczmarek LK.** Activation of a calcium entry pathway by sodium pyridithione in the bag cell neurons of *Aplysia*. *J Neurobiol* 60: 411–423, 2004.
- Knox RJ, Quattrochi EA, Connor JA, Kaczmarek LK.** Recruitment of Ca²⁺ channels by protein kinase C during rapid formation of putative neuropeptide release sites in isolated *Aplysia* neurons. *Neuron* 8: 883–889, 1992.
- Kupfermann I, Kandel ER.** Electrophysiological properties and functional interconnections of two symmetrical neurosecretory clusters (bag cells) in abdominal ganglion of *Aplysia*. *J Neurophysiol* 33: 865–876, 1970.
- Laird DW.** Connexin phosphorylation as a regulatory event linked to gap junction internalization and degradation. *Biochim Biophys Acta* 1711: 172–182, 2005.
- Lampe PD, Lau AF.** The effects of connexin phosphorylation on gap junctional communication. *Int J Biochem Cell Biol* 36: 1171–1186, 2004.
- Lampe PD, TenBroek EM, Burt JM, Kurata WE, Johnson RG, Lau AF.** Phosphorylation of connexin43 on serine368 by protein kinase C regulates gap junctional communication. *J Cell Biol* 149: 1503–1512, 2000.
- Landisman CE, Connors BW.** Long-term modulation of electrical synapses in the mammalian thalamus. *Science* 310: 1809–1813, 2005.
- Landisman CE, Long MA, Beierlein M, Deans MR, Paul DL, Connors BW.** Electrical synapses in the thalamic reticular nucleus. *J Neurosci* 22: 1002–1009, 2002.
- Lazrak A, Peracchia C.** Gap junction gating sensitivity to physiological internal calcium regardless of pH in Novikoff hepatoma cells. *Biophys J* 65: 2002–2012, 1993.
- Lazrak A, Peres A, Giovannardi S, Peracchia C.** Ca²⁺-mediated and independent effects of arachidonic acid on gap junctions and Ca²⁺-independent effects of oleic acid and halothane. *Biophys J* 67: 1052–1059, 1994.
- Levitan IB.** It is calmodulin after all! Mediator of the calcium modulation of multiple ion channels. *Neuron* 22: 645–648, 1999.
- Locco D, Thompson C, Tobe S.** Intercellular communication in an insect endocrine gland. *J Exp Biol* 121: 407–419, 1986.
- Loewenstein WR, Nakas M, Socolar SJ.** Junctional membrane uncoupling. Permeability transformations at a cell membrane junction. *J Gen Physiol* 50: 1865–1891, 1967.
- Magoski NS, Knox RJ, Kaczmarek LK.** Activation of a Ca²⁺ permeable cation channel produces a prolonged attenuation of intracellular Ca²⁺ release in *Aplysia* bag cell neurons. *J Physiol* 522: 271–283, 2000.
- Meissner G.** Ryanodine activation and inhibition of the Ca²⁺ release channel of sarcoplasmic reticulum. *J Biol Chem* 261: 6300–6306, 1985.

- Michel S, Wayne NL.** Neurohormone secretion persists after post-afterdischarge membrane depolarization and cytosolic calcium elevation in peptidergic neurons in intact nervous tissue. *J Neurosci* 22: 9063–9069, 2002.
- Moreno AP, Lau AF.** Gap junction channel gating modulated through protein phosphorylation. *Prog Biophys Mol Biol* 94: 107–119, 2007.
- Moreno AP, Saez JC, Fishman GI, Spray DC.** Human connexin43 gap junction channels. Regulation of unitary conductances by phosphorylation. *Circ Res* 74: 1050–1057, 1994.
- Mustonen H, Kiviluoto T, Paimela H, Puolakkainen P, Kivilaakso E.** Calcium signaling is involved in ethanol induced volume decrease and gap junction closure in cultured rat gastric mucosal cells. *Dig Dis Sci* 50: 103–110, 2005.
- Nakanishi K, Zhang F, Baxter DA, Eskin A, Byrne JH.** Role of calcium-calmodulin-dependent protein kinase II in modulation of sensorimotor synapses in *Aplysia*. *J Neurophysiol* 78: 409–416, 1997.
- Naraghi M.** T-jump study of calcium binding kinetics of calcium chelators. *Cell Calcium* 22: 255–68, 1997.
- Neyton J, Trautmann A.** Physiological modulation of gap junction permeability. *J Exp Biol* 124: 93–114, 1986.
- Peracchia C.** Calmodulin-like proteins and communicating junctions. Electrical uncoupling of crayfish septate axons is inhibited by the calmodulin inhibitor W7 and is not affected by cyclic nucleotides. *Pflügers Arch* 408: 379–385, 1987.
- Peracchia C.** Increase in gap junction resistance with acidification in crayfish septate axons is closely related to changes in intracellular calcium but not hydrogen ion concentration. *J Membr Biol* 113: 75–92, 1990.
- Peracchia C.** Chemical gating of gap junction channels: roles of calcium, pH and calmodulin. *Biochim Biophys Acta* 1662: 61–80, 2004.
- Peracchia C, Bernardini G, Peracchia LL.** Is calmodulin involved in the regulation of gap junction permeability? *Pflügers Arch* 399: 152–154, 1983.
- Peracchia C, Dulhunty AF.** Low resistance junctions in crayfish. Structural changes with functional uncoupling. *J Cell Biol* 70: 419–439, 1976.
- Peracchia C, Sotkis A, Wang XG, Peracchia LL, Persechini A.** Calmodulin directly gates gap junction channels. *J Biol Chem* 275: 26220–26224, 2000.
- Pereda AE, Bell TD, Chang BH, Czernik AJ, Nairn AC, Soderling TR, Faber DS.** Ca²⁺/calmodulin-dependent kinase II mediates simultaneous enhancement of gap-junctional conductance and glutamatergic transmission. *Proc Natl Acad Sci USA* 95: 13272–13277, 1998.
- Pinsker HM, Dudek FE.** Bag cell control of egg laying in freely behaving *Aplysia*. *Science* 197: 490–493, 1977.
- Potenza N, del Gaudio R, Riviaccio L, Russo GM, Geraci G.** Cloning and molecular characterization of the first innexin of the phylum Annelida—expression of the gene during development. *J Mol Evol* 54: 312–321, 2002.
- Rao G, Barnes CA, McNaughton BL.** Occlusion of hippocampal electrical junctions by intracellular calcium injection. *Brain Res* 408: 267–270, 1987.
- Rohr R.** Role of gap junctions in the propagation of the cardiac action potential. *Cardiovasc Res* 62: 309–322, 2004.
- Rose B, Loewenstein WR.** Calcium ion distribution in cytoplasm visualised by aequorin: diffusion in cytosol restricted by energized sequestering. *Science* 190: 1204–1206, 1975.
- Rose B, Loewenstein WR.** Permeability of a cell junction and the local cytoplasmic free ionized calcium concentration: a study with aequorin. *J Membr Biol* 28: 87–119, 1976.
- Rothman BS, Weir G, Dudek FE.** Egg-laying hormone: direct action on the ovotestis of *Aplysia*. *Gen Comp Endocrinol* 52: 134–141, 1983.
- Saez JC, Connor JA, Spray DC, Bennett MV.** Hepatocyte gap junctions are permeable to the second messenger, inositol 1,4,5-trisphosphate, and to calcium ions. *Proc Natl Acad Sci USA* 86: 2708–2712, 1989.
- Saez JC, Narin AC, Czernik AJ, Spray DC, Hertzberg EL, Greengard P, Bennett MV.** Phosphorylation of connexin 32, a hepatocyte gap-junction protein, by cAMP-dependent protein kinase, protein kinase C and Ca²⁺/calmodulin-dependent protein kinase II. *Eur J Biochem* 192: 263–273, 1990.
- Schirrmacher K, Nonhoff D, Wiemann M, Peterson-Grine E, Brink PR, Bingmann D.** Effects of calcium on gap junctions between osteoblast-like cells in culture. *Calcif Tissue Int* 59: 259–264, 1996.
- Seidler NW, Jona I, Vegh M, Martonosi A.** Cyclopiazonic acid is a specific inhibitor of the Ca²⁺-ATPase of sarcoplasmic reticulum. *J Biol Chem* 264: 17816–17823, 1989.
- Söhl G, Maxeiner S, Willecke K.** Expression and functions of neuronal gap junctions. *Nat Rev Neurosci* 6: 191–200, 2005.
- Sohl G, Willecke K.** Gap junctions and the connexin protein family. *Cardiovasc Res* 62: 228–232, 2004.
- Solan JL, Lampe PD.** Connexin phosphorylation as a regulatory event linked to gap junction channel assembly. *Biochim Biophys Acta* 1711: 154–163, 2005.
- Sossin WS, Diaz-Arrastia R, Schwartz JH.** Characterization of two isoforms of protein kinase C in the nervous system of *Aplysia californica*. *J Biol Chem* 268: 5763–5768, 1993.
- Sossin WS, Schwartz JH.** Selective activation of Ca²⁺-activated PKCs in *Aplysia* neurons by 5-HT. *J Neurosci* 12: 1160–1168, 1992.
- Spray DC, Bennett MV.** Physiology and pharmacology of gap junctions. *Annu Rev Physiol* 47: 281–303, 1985.
- Spray DC, Stern JH, Harris AL, Bennett MV.** Gap junctional conductance: comparison of sensitivities to H and Ca ions. *Proc Natl Acad Sci USA* 79: 441–445, 1982.
- Sumi M, Kiuchi K, Ishikawa T, Ishii A, Hagiwara M, Nagatsu T, Hidaka H.** The newly synthesized selective Ca²⁺/calmodulin dependent protein kinase II inhibitor KN-93 reduces dopamine contents in PC12h cells. *Biochem Biophys Res Commun* 181: 968–975, 1991.
- Tam AK, Gardam KE, Lamb S, Kachoei BA, Magoski NS.** Role for protein kinase C in controlling *Aplysia* bag cell neuron excitability. *Neuroscience* 179: 41–55, 2011.
- Tam AK, Geiger JE, Hung AY, Groten CJ, Magoski NS.** Persistent Ca²⁺ current contributes to a prolonged depolarization in *Aplysia* bag cell neurons. *J Neurophysiol* 102: 3753–3765, 2009.
- Thastrup O, Cullen PJ, Dröbak BK, Hanley MR, Dawson AP.** Thapsigargin, a tumor promoter, discharges intracellular Ca²⁺ stores by specific inhibition of the endoplasmic reticulum Ca²⁺-ATPase. *Proc Natl Acad Sci USA* 87: 2466–2470, 1990.
- Tokumitsu H, Chijiwa T, Hagiwara M, Mizutani A, Terasawa M, Hidaka H.** KN-62, 1-[N,O-bis(5-isoquinolinesulfonyl)-N-methyl-L-tyrosyl]-4-phenylpiperazine, a specific inhibitor of Ca²⁺/calmodulin-dependent protein kinase II. *J Biol Chem* 265: 4315–4320, 1990.
- Toyama J, Sugiura H, Kamiya K, Kodama I, Terasawa M, Hidaka H.** Ca²⁺-calmodulin mediated modulation of the electrical coupling of ventricular myocytes isolated from guinea pig heart. *J Mol Cell Cardiol* 26: 1007–1015, 1994.
- Traub RD, Kopell N, Bibbig A, Buhl EH, LeBeau FE, Whittington MA.** Gap junctions between interneuron dendrites can enhance synchrony of gamma oscillations in distributed networks. *J Neurosci* 21: 9478–9486, 2001.
- Van Eldik LJ, Hertzberg EL, Berdan RC, Gilulz NB.** Interaction of calmodulin and other calcium-modulated proteins with mammalian and arthropod junctional membrane proteins. *Biochem Biophys Res Commun* 126: 825–832, 1985.
- van Veen TA, van Rijen HV, Jongsma HJ.** Electrical conductance of mouse connexin45 gap junction channels is modulated by phosphorylation. *Cardiovasc Res* 46: 496–510, 2000.
- Vorndran C, Minta A, Poenie M.** New fluorescent calcium indicators designed for cytosolic retention or measuring calcium near membranes. *Biophys J* 69: 2112–2124, 1995.
- Wayman GA, Lee YS, Tokumitsu H, Silva A, Soderling TR.** Calmodulin-kinases: modulators of neuronal development and plasticity. *Neuron* 59: 914–931, 2008.
- Wayne NL, Lee W, Kim YJ.** Persistent activation of calcium-activated and calcium-independent protein kinase C in response to electrical afterdischarge from peptidergic neurons of *Aplysia*. *Brain Res* 834: 211–213, 1999.
- White RL, Doeller JE, Verselis VK, Wittenberg BA.** Gap junctional conductance between pairs of ventricular myocytes is modulated synergistically by H⁺ and Ca²⁺. *J Gen Physiol* 95: 1061–1075, 1990.
- White SH, Magoski NS.** Acetylcholine-evoked afterdischarge in *Aplysia* bag cell neurons. *J Neurophysiol* 107: 2672–2685, 2012.